Thin–Walled Structures 209 (2025) 112949

Contents lists available at ScienceDirect

Thin-Walled Structures

journal homepage: www.elsevier.com/locate/tws

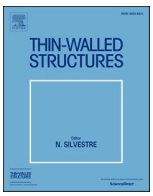

Full length article

A modified spectral collocation method for vibration of sandwich beams based on a higher-order layer-wise beam theory

Ming Ji [a,*], Yu Sekiguchi [a], Masanobu Naito [b], Chiaki Sato [a]

[a] Institute of Integrated Research, Institute of Science Tokyo, 4259 Nagatsuta cho, Midoriku, Yokohama 226-8501, Japan
[b] Research Center for Macromolecules and Biomaterials, National Institute for Materials Science (NIMS), Ibaraki 305-0047 Japan

ARTICLE INFO

Keywords:
Modified spectral collocation method
Viscoelastic core
Higher-order layer-wise beam theory
Sandwich beam

ABSTRACT

This paper studied vibration characteristics of sandwich beams with viscoelastic cores and different boundary conditions. A higher-order layer-wise beam theory was presented to describe the displacement field of the sandwich beams with viscoelastic cores. The top and bottom layers' transverse shear stresses were thought to be quadratic. And the viscoelastic core's transverse shear stress was constant. It was believed that the transverse shear stress and displacement at the layer interface are continuous. The equations of motion and boundary conditions were established using Hamilton's principle. A modified spectral collocation method was utilized to solve the equations of motion with various boundary conditions by combining the integrated-based spectral collocation method and conventional spectral collocation method. The modified method can implement multiple boundary conditions at one boundary point. An iterative procedure was utilized to solve complex eigenvalue problem with frequency-dependent material properties. The accuracy of the proposed method was verified by contrasting the theoretical data with experimental and published data. Tensile test was conducted to obtain the Poisson's ratio of adhesive using Digital Image Correlation (DIC). The storage and loss modulus of adhesive were measured using Oberst beam. Impact tests were conducted to estimate resonant frequencies and loss factors of sandwich beams from Impulse response function (IRF). The measured results agreed well with the data calculated using the proposed method.

1. Introduction

Noise, vibration, fatigue may lead to serious problems in structures subjected to dynamic loadings. Thus, reducing the vibration is crucial in the design of machines. The soft, viscoelastic materials are good choice to dissipate vibration energy. Hence, it is essential to estimate the dynamic characteristics of the sandwich structures precisely. To date, there have been considerable research on the topic [1–3].

Some significant early developments to the free vibration of sandwich beams with viscoelastic cores are by made by Kerwin [4], DiTaranto [5], DiTaranto and Blasingame [6], Mead and Markus [7,8]. DiTaranto [5] obtained a sixth-order ordinary differential equation in terms of in-plane displacement for sandwich beams with viscoelastic cores based on Kerwin's assumptions [4], and gave the analytical solutions for finite beams with various boundary conditions [6]. Then, Mead and Markus [7,8] derived the same equation in terms of lateral displacement. Following Mead and Markus, Rao [9] derived the same equation using energy approach, and calculated the responses of sandwich beams subject to moving loads [10]. Hyer et al. [11] gave approximate equations for nonlinear vibration of sandwich beams. Oravský et al. [12] proposed an approximation method to estimate the sandwich beams' loss factors. Lifshitz and Leibowitz [13] applied the sixth-order ordinary differential equation in optimal design of damping sandwich beams. Ioannides and Grootenhuis [14] gave an integral equation for sandwich beams based on the same assumptions. He and Rao [15] utilized Rayleigh-Ritz approach to address the curved sandwich beams' vibration. Fasana and Marchesiello [16] analyzed the dynamic issues of sandwich beams with three damped layers using Rayleigh-Ritz approach. Sisemore and Darvennes [17] investigated the compression effect of the viscoelastic core on the sandwich beams' free vibration. Cai et al. [18] used Rayleigh-Ritz approach to solve the free vibration of beams with partial passive constrained layer damping. Khalili et al. [19] proposed an improved dynamic stiffness method for symmetric sandwich beams. Arikoglu and Ozkol [20] used differential transform method to inspect the free vibration of sandwich beams. Hamdaoui et al. [21] used a multi-objective optimization method in

* Corresponding author.
E-mail address: ji.m.aa@m.titech.ac.jp (M. Ji).

https://doi.org/10.1016/j.tws.2025.112949
Received 25 October 2024; Received in revised form 11 December 2024; Accepted 12 January 2025
Available online 13 January 2025

optimal design of sandwich beams for loss mass and high damping. Hamdaoui et al. [22] developed an adjoint method to determine viscoelastic material properties by comparing the loss factors and frequencies determined from finite element method and experiments. The above researches assumed that the displacement fields of the layers were layer-wise and the two elastic beams were based on Euler-Bernoulli beam theory. Rao [23] analyzed the free vibration of short unsymmetric sandwich beams based on the first-order beam theory. Mead and Markus [24] used the first-order layer-wise beam theory to analyze the coupled vibration of sandwich beams. Rikards [25] applied finite element method to analyze vibration and damping for sandwich beams. Each layer's displacement was based on Timoshenko beam theory. Lam and Chun [26] gave the analytical solutions for the dynamic responses of a sandwich beam with simply-supported boundary conditions subject to an impulse loading. The effect of rotary inertia and transverse shear deformation in each layer were considered. Ganapathi et al. [27] investigated the linear and nonlinear dynamics of sandwich and composite beams using the finite element method. The transverse shear deformation was assumed to be trigonometric sine function. Plagianakos and Saravanos [28] created a high-order layer-wise beam theory based finite element to estimate the damping of composite laminated sandwich beams. Tahani [29] presented two layer-wise beam theories to explore the static and dynamic responses of laminated composite beams. Arvin et al. [30] showed a higher order layer-wise beam theory for sandwich composite beams. The transverse displacements in elastic layers were independent, and the variable in the core layer was linear along the thickness direction. Loja et al. [31] explored the free vibration of sandwich beams using different layer-wise theories and kriging-based finite element method. Ren and Zhao [32] proposed a layer-wise beam theory with continuous transverse shear stress for sandwich beams with soft core.

For the simple layer-wise beam theories, it is possible to get the analytical solutions for the vibration and damping of sandwich beams with viscoelastic cores. However, it is difficult to get the analytical or semi-analytical solutions for the higher-order layer-wise theories of sandwich beams with diverse boundary conditions. Most studies utilized the finite element method to solve the problem. Spectral method is a powerful tool to solve the problems [33]. The spectral collocation method has been widely used in fluid mechanics [34–36] and solid mechanics [37–41]. Mattei [42] used the Tchebycheff collocation method to investigate the vibration and acoustic radiation of fluid-loaded baffled plates. Sari et al. investigated the effect of damaged boundaries on the vibration of rectangular plates using Mindlin plate theory [43] and Kirchhoff plate theory [44]. Wang and Huang [45] employed the Chebyshev collocation method to study the acoustic wave propagation. Mohazzab [46] investigated the vibration of composite laminated plates and shells using the spectral collocation method. Mohazzab and Dozio [47] investigated in-plane vibration of skew plates. Xie et al. [48] presented an integral method to study the free vibration of coupled shells. Ji et al. [40] investigated the free vibration and transient responses of fluid-loaded plates subjected to impact loadings. Ji et al. [41] investigated the transient responses of cantilever plates subjected normal and oblique impact loadings, and estimate the impact force history inversely. Above all, few researches focus on the vibration of layered structures using spectral collocation method. Tossapanon and Wattanasakulpong studied the stability and vibration of functionally graded beams [49] and plates [50] using the spectral collocation method. Dong et al. [51] applied Chebyshev polynomials and Ritz method to solve the travelling wave vibrations of a moderately thick cylindrical shell subject to a spinning motion. Then, they [52] utilized the similar method to deal with the coupled multi-mode vibrations of cylindrical shells. Ji et al. [53] investigated the vibration of sandwich plates using spectral collocation method and layer-wise plate theory. Fernandes et al. [54] developed a layer-wise shallow shell theory taking both translational and rotational effect into consideration to solve the static and free vibration of thin and thick cross-ply laminated shells. The radial basis function collocation methods in pseudospectral form were used to solve the associated equations. Tornabene et al. [55] utilized the Equivalent Layer Wise (ELW) method to derive the balance equations of the hygro-thermo-magneto-electro-elastic problem for laminated doubly-curved shells. The Generalized Differential Quadrature (GDQ) numerical method was applied to solve the balance equations. Tornabene et al. [56] applied higher order Equivalent Layer-Wise formulation to derive the thermo-mechanical governing equations of laminated doubly-curved shells. The Fourier-based Generalized Differential Quadrature (F-GDQ) and Taylor-based Generalized Integral Quadrature (GTIQ) were adopted to calculate the governing equations numerically.

Attempting to handle the problem of the free vibration and damping of sandwich beams containing viscoelastic cores using the spectral collocation method is a challenging task, especially dealing with the various boundary conditions. Thus, a higher-order layer-wise beam theory was utilized to study the vibration characteristics of sandwich beams containing viscoelastic cores. It was believed that the transverse shear stress and displacement at the layer interface would be continuous. The equations of motion and boundary conditions were established using Hamilton's principle. A modified spectral collocation method was utilized to solve the equations of motion with various boundary conditions by combining the integrated-based spectral collocation method and conventional spectral collocation method. The modified method can implement multiple boundary conditions at one boundary point. An iterative procedure was utilized to solve complex eigenvalue problem with frequency-dependent material properties. The accuracy of the proposed method was verified by contrasting the theoretical data with experimental and published data. The measured results agreed well with the data calculated using the proposed method. The proposed method should be of use to researchers and designers to reduce the vibration and noise of sandwich beams with various boundary conditions using viscoelastic materials.

2. Higher-order layer-wise beam theory

A sandwich beam containing a viscoelastic core is shown in Fig. 1. The length and width are represented by L and b, respectively. The h^t denotes the top layer's thickness, h^c denotes the core layer's thickness, and h^b denotes the bottom layer's thickness. The total thickness of the sandwich beam is defined as $h = h^t + h^c + h^b$. The x, y, z-axis are along the length, width, and thickness directions of the beam, respectively. The assumptions for the higher order layer-wise beam theory are as follows:

(1) The sandwich beam's neutral axis moves in a frequency-dependent manner.
(2) The materials are taken to be homogenous and isotropic. The bonded materials are linearly elastic, and the core's material is viscoelastic.
(3) The transverse displacements are the same.
(4) There is no slipping at the layer interface, and the transverse shear stresses are continuous.
(5) The elastic layers' transverse shear stresses are quadratic, and the viscoelastic layer's transverse shear stress is constant.

The displacement field is described by [32,67]

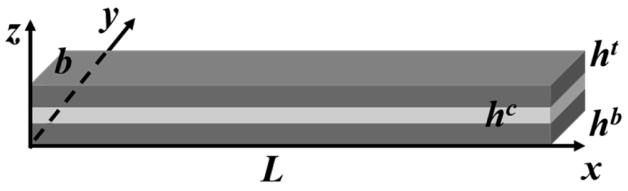

Fig. 1. Schematic of a sandwich beam containing a viscoelastic core.

$$u(x,z) = u_0^c(x) - z\frac{\partial w_0(x)}{\partial x} + l(z)\beta^c(x) + m(z)\phi^t(x) + n(z)\phi^b(x), \tag{1}$$

$$w(x,z) = w_0(x). \tag{2}$$

The functions in the displacement field are

$$l(z) = \begin{cases} \mathrm{H}^t(z) - \mathrm{H}^t(z_{t_2}) + z_{t_2}, z \in \left[\frac{h^c}{2}, \frac{h^c}{2} + h^t\right] \\ z,\ z \in \left[-\frac{h^c}{2}, \frac{h^c}{2}\right] \\ \mathrm{H}^b(z) - \mathrm{H}^b(z_{b_1}) + z_{b_1}, z \in \left[-\frac{h^c}{2} - h^b, -\frac{h^c}{2}\right] \end{cases}, \tag{3}$$

$$m(z) = \begin{cases} \Gamma^t(z) - \Gamma^t(z_{t_2}), z \in \left[\frac{h^c}{2}, \frac{h^c}{2} + h^t\right] \\ 0, z \in \left[-\frac{h^c}{2} - h^b, \frac{h^c}{2}\right] \end{cases}, \tag{4}$$

$$n(z) = \begin{cases} 0, z \in \left[-\frac{h^c}{2}, \frac{h^c}{2} + h^t\right] \\ \Gamma^b(z) - \Gamma^b(z_{b_1}), z \in \left[-\frac{h^c}{2} - h^b, -\frac{h^c}{2}\right] \end{cases}, \tag{5}$$

where u_0^c is the in-plane displacement at the middle surface of the core; β^c is the core's slope of the normal; ϕ^t and ϕ^b are top and bottom's third order displacements, respectively; w_0 is the transverse displacement; $\mathrm{H}^t(z) = \frac{\left(2z_{t_1}z - z^2\right)G^c}{2h^tG^t}$; $\mathrm{H}^b(z) = \frac{\left(z^2 - 2z_{b_2}z\right)G^c}{2h^bG^b}$; $\Gamma^t(z) = \frac{2z^3 - 3\left(z_{t_2}+z_{t_1}\right)z^2 + 6z_{t_1}z_{t_2}z}{6h^t}$; $\Gamma^b(z) = \frac{2z^3 - 3\left(z_{b_2}+z_{b_1}\right)z^2 + 6z_{b_1}z_{b_2}z}{6h^b}$; $z_{t_1} = \frac{h^c}{2} + h^t$; $z_{t_2} = \frac{h^c}{2}$; $z_{b_1} = -\frac{h^c}{2}$; $z_{b_2} = -\frac{h^c}{2} + h^b$; the superscript '$t$' means top, '$c$' means core, and '$b$' means bottom; G represents the shear modulus. The strains can be given by

$$\varepsilon_x = \frac{\partial u}{\partial x},\ \gamma_{xz} = \frac{\partial u}{\partial z} + \frac{\partial w}{\partial x}. \tag{6}$$

The stress-strain relationship is expressed as

$$\sigma_x^k = E^k\varepsilon_x^k,\ \tau_{xz}^k = G^k\gamma_{xz}^k, \tag{7}$$

where E is the Young's modulus; the superscript means the k layer (k= t, c or b) of the sandwich beam. The sandwich beam's equations of motion, which take into account kinetic energy and potential energy, are obtained using Hamilton's principle [51,52,57–60].

$$\delta T - \delta V = 0, \tag{8}$$

$$T = \sum_{k=t,c,b}\frac{\rho^k}{2}\int_{t_0}^{t_1}\int_{\Omega^k}\left(\left(\frac{\partial u}{\partial t}\right)^2 + \left(\frac{\partial w}{\partial t}\right)^2\right)\mathrm{d}\Omega^k\mathrm{d}t, \tag{9}$$

$$V = \sum_{k=t,c,b}\frac{1}{2}\int_{t_0}^{t_1}\int_{\Omega^k}\left(\sigma_x^k\varepsilon_x^k + \tau_{xz}^k\gamma_{xz}^k\right)\mathrm{d}\Omega^k\mathrm{d}t, \tag{10}$$

where T is the kinetic energy and V is potential energy; t is time; Ω is the geometric domain; ρ is the density. The equations of motions are expressed as

$$\frac{\partial N_x^t}{\partial x} + \frac{\partial N_x^c}{\partial x} + \frac{\partial N_x^b}{\partial x} = I_{11}\frac{\partial^2 u_0^c}{\partial t^2} + I_{12}\frac{\partial^3 w_0}{\partial x\partial t^2} + I_{13}\frac{\partial^2\beta^c}{\partial t^2} + I_{14}\frac{\partial^2\phi^t}{\partial t^2} + I_{15}\frac{\partial^2\phi^b}{\partial t^2}, \tag{11}$$

$$\begin{aligned}\frac{\partial^2 M_x^t}{\partial x^2} + \frac{\partial^2 M_x^c}{\partial x^2} + \frac{\partial^2 M_x^b}{\partial x^2} &= I_{12}\frac{\partial^3 u_0^c}{\partial x\partial t^2} + I_{11}\frac{\partial^2 w_0}{\partial t^2} \\ &+ I_{22}\frac{\partial^4 w_0}{\partial x^2\partial t^2} + I_{23}\frac{\partial^3\beta^c}{\partial x\partial t^2} + I_{24}\frac{\partial^3\phi^t}{\partial x\partial t^2} + I_{25}\frac{\partial^3\phi^b}{\partial x\partial t^2}\end{aligned}, \tag{12}$$

$$\begin{aligned}&\frac{\partial P_x^t}{\partial x} + \frac{\partial M_x^c}{\partial x} + \frac{\partial P_x^b}{\partial x} - R_{xz}^t - R_{xz}^c - R_{xz}^b = \\ &I_{13}\frac{\partial^2 u_0^c}{\partial t^2} + I_{23}\frac{\partial^3 w_0}{\partial x\partial t^2} + I_{33}\frac{\partial^2\beta^c}{\partial t^2} + I_{34}\frac{\partial^2\phi^t}{\partial t^2} + I_{35}\frac{\partial^2\phi^b}{\partial t^2}\end{aligned}, \tag{13}$$

$$\frac{\partial Q_x^t}{\partial x} - S_{xz}^t = I_{14}\frac{\partial^2 u_0^c}{\partial t^2} + I_{24}\frac{\partial^3 w_0}{\partial x\partial t^2} + I_{23}\frac{\partial^2\beta^c}{\partial t^2} + I_{44}\frac{\partial^2\phi^t}{\partial t^2}, \tag{14}$$

$$\frac{\partial Q_x^b}{\partial x} - S_{xz}^b = I_{15}\frac{\partial^2 u_0^c}{\partial t^2} + I_{25}\frac{\partial^3 w_0}{\partial x\partial t^2} + I_{25}\frac{\partial^2\beta^c}{\partial t^2} + I_{55}\frac{\partial^2\phi^b}{\partial t^2}. \tag{15}$$

The variables of force and moment terms in Eqs. (11) through (15) are expressed in Eq. (A.1) in the Appendix. And the parameters of the inertia in Eqs. (11) through (15) are expressed in Eqs. (A.2) through (A.5) in the Appendix. The essential boundary conditions (fixed) are described as

$$u_0^c = w_0 = \frac{\partial w_0}{\partial x} = \beta^c = \phi^t = \phi^b = 0, \tag{16}$$

The corresponding natural boundary conditions (free) are described as

$$\begin{aligned}&N_x^t + N_x^c + N_x^b = M_x^t + M_x^c + M_x^b \\ &+I_{12}\frac{\partial^3 u_0^c}{\partial x\partial t^2} + I_{22}\frac{\partial^3 w_0}{\partial x\partial t^2} - I_{23}\frac{\partial^2\beta^c}{\partial t^2} - I_{24}\frac{\partial^2\phi^t}{\partial t^2} - I_{25}\frac{\partial^2\phi^b}{\partial t^2} \\ &= \frac{\partial M_x^t}{\partial x} + \frac{\partial M_x^c}{\partial x} + \frac{\partial M_x^b}{\partial x} = P_x^t + M_x^c + P_x^b = Q_x^t = Q_x^b = 0.\end{aligned} \tag{17}$$

3. Modified spectral collocation method

A fast numerical method known as the spectral collocation method is employed to solve the equations of motion with boundary conditions. A grid of Gauss-Chebyshev-Lobatto points in the interval [−1, 1] is introduced [33]. Thus, it is necessary to transfer the coordinate x to interval [−1, 1] with the relationship $\xi = \frac{2x}{L} - 1$. However, there is a problem using the conventional spectral collocation method when solving the equations. For the variable w_0, there are two boundary conditions at each boundary. However, only one boundary condition can be imposed at one node. To overcome the problem, a boundary condition is imposed at the boundary node and another at the node next to the boundary node [61]. Although the procedure is simple to use, it is not exact. Mai-Duy [62] proposed an integration-based spectral collocation method to handle the problem effectively. It proved that the proposed integration-based spectral collocation method provides more accurate results and faster convergence. Thus, the modified spectral collocation method is developed to solve the free vibration problem of sandwich beams based on a higher-order layer-wise beam theory by combining the integration-based spectral collocation method for the variable w_0 and the conventional spectral collocation method for the variables $u_0^c, \beta^c, \phi^t, \phi^b$. The subsequent non-dimensional variables are explained.

$$\overline{u}_0^c = \frac{u_0^c}{h}, \overline{w}_0 = \frac{w_0}{h}, \overline{\beta}^c = \beta^c, \overline{\phi}^t = h\phi^t, \overline{\phi}^b = h\phi^b. \tag{18}$$

The conventional spectral collocation method is applied to the variables $\overline{u}_0^c, \overline{\beta}^c, \overline{\phi}^t, \overline{\phi}^b$. The Chebyshev differentiation matrix is described as $\mathbf{D}_1$ [33]; the second-order differentiation matrix is expressed as $\mathbf{D}_2 = (\mathbf{D}_1)^2$, and so on for the higher-order differentiation matrix. The fourth-order derivative $\mathrm{d}^4\overline{w}_0/\mathrm{d}\xi^4$ is approximated as

$$\frac{\mathrm{d}^4\overline{w}_0}{\mathrm{d}\xi^4} = \sum_{k=0}^{N} a_k T_k(\xi), \tag{19}$$

where $T_k(\xi)$ is Chebyshev polynomial of first kind.

$$\frac{\mathrm{d}^3\overline{w}_0}{\mathrm{d}\xi^3}=\sum_{k=0}^{N}a_k I_k^{(3)}(\xi)+c_1, \tag{20}$$

$$\frac{\mathrm{d}^2\overline{w}_0}{\mathrm{d}\xi^2}=\sum_{k=0}^{N}a_k I_k^{(2)}(\xi)+c_1\xi+c_2, \tag{21}$$

$$\frac{\mathrm{d}\overline{w}_0}{\mathrm{d}\xi}=\sum_{k=0}^{N}a_k I_k^{(1)}(\xi)+\frac{1}{2}c_1\xi^2+c_2\xi+c_3, \tag{22}$$

$$\overline{w}_0=\sum_{k=0}^{N}a_k I_k^{(0)}(\xi)+\frac{1}{6}c_1\xi^3+\frac{1}{2}c_2\xi^2+c_3\xi+c_4, \tag{23}$$

where $I_k^{(3)}(\xi)=\int T_k(\xi)\mathrm{d}\xi$, $I_k^{(2)}(\xi)=\int I_k^{(3)}(\xi)\mathrm{d}\xi$, $I_k^{(1)}(\xi)=\int I_k^{(2)}(\xi)\mathrm{d}\xi$, $I_k^{(0)}(\xi)=\int I_k^{(1)}(\xi)\mathrm{d}\xi$, and c_1-c_4 are four unknown constants. The jth-order differentiation matrix is described as $\mathbf{D}_{ij}$, whose size is $(N+1)\times(N+5)$. The unknown vector is $[a_0 \quad a_1 \quad \cdots \quad a_N \quad c_1 \quad c_2 \quad c_3 \quad c_4]^T$. Thus, the unknown vector at the $N+1$ collocation points is defined as

$$\begin{aligned}\mathbf{U}=\big[&\overline{u}^c_{0,0} \quad \cdots \quad \overline{u}^c_{0,N} \quad a_0 \quad \cdots \quad a_N \quad c_1 \quad \cdots \quad c_4\\ &\overline{\beta}^c{}_{,0} \quad \cdots \quad \overline{\beta}^c{}_{,N} \quad \overline{\phi}^t{}_{,0} \quad \cdots \quad \overline{\phi}^t{}_{,N} \quad \overline{\phi}^b{}_{,0} \quad \cdots \quad \overline{\phi}^b{}_{,N}\big]^T,\end{aligned} \tag{24}$$

where the superscript "T" means "transpose". Then, the sandwich beam is assumed to vibrate at the angular frequency ω. The equations of motion in Eqs. (11) through (15) can be written in the following forms based on the mixed differentiation matrix.

$$\begin{bmatrix}\mathbf{L}_{11}&\mathbf{L}_{12}&\mathbf{L}_{13}&\mathbf{L}_{14}&\mathbf{L}_{15}\\ \mathbf{L}_{21}&\mathbf{L}_{22}&\mathbf{L}_{23}&\mathbf{L}_{24}&\mathbf{L}_{25}\\ \mathbf{L}_{31}&\mathbf{L}_{32}&\mathbf{L}_{33}&\mathbf{L}_{34}&\mathbf{L}_{35}\\ \mathbf{L}_{41}&\mathbf{L}_{42}&\mathbf{L}_{43}&\mathbf{L}_{44}&\mathbf{L}_{45}\\ \mathbf{L}_{51}&\mathbf{L}_{52}&\mathbf{L}_{53}&\mathbf{L}_{54}&\mathbf{L}_{55}\end{bmatrix}\mathbf{U}=\omega^2\begin{bmatrix}\mathbf{R}_{11}&\mathbf{R}_{12}&\mathbf{R}_{13}&\mathbf{R}_{14}&\mathbf{R}_{15}\\ \mathbf{R}_{21}&\mathbf{R}_{22}&\mathbf{R}_{23}&\mathbf{R}_{24}&\mathbf{R}_{25}\\ \mathbf{R}_{31}&\mathbf{R}_{32}&\mathbf{R}_{33}&\mathbf{R}_{34}&\mathbf{R}_{35}\\ \mathbf{R}_{41}&\mathbf{R}_{42}&\mathbf{R}_{43}&\mathbf{R}_{44}&\mathbf{R}_{45}\\ \mathbf{R}_{51}&\mathbf{R}_{52}&\mathbf{R}_{53}&\mathbf{R}_{54}&\mathbf{R}_{55}\end{bmatrix}\mathbf{U}, \tag{25}$$

where the terms in the matrix are expressed in Eqs. (A.6) through (A.15) in the Appendix. The boundary conditions are defined. Here the free-free boundary conditions are defined as an example. From the Hamilton's principle, the natural boundary conditions mean the free boundary conditions. The conditions at $x=0$ can be expressed as

$$\begin{bmatrix}C_{11}\frac{2h}{L}\mathbf{D}_1(N+1,:) & C_{12}\frac{4h}{L^2}\mathbf{D}_{12}(N+1,:) & C_{13}\frac{2}{L}\mathbf{D}_1(N+1,:)\\ -C_{14}\frac{2}{Lh}\mathbf{D}_1(N+1,:) & C_{15}\frac{2}{Lh}\mathbf{D}_1(N+1,:)\end{bmatrix}\mathbf{U}=0, \tag{26}$$

$$\begin{aligned}&\Big[-C_{12}\frac{4h}{L^2}\mathbf{D}_2(N+1,:) \quad -C_{22}\frac{8h}{L^3}\mathbf{D}_{13}(N+1,:) \quad C_{23}\frac{4}{L^2}\mathbf{D}_2(N+1,:)\\ &-C_{24}\frac{4}{L^2h}\mathbf{D}_2(N+1,:) \quad -C_{25}\frac{4}{L^2h}\mathbf{D}_2(N+1,:)\Big]\mathbf{U}=\\ &\omega^2\Big[I_{12}h\mathbf{I}(N+1,:) \quad -I_{22}\frac{2h}{L}\mathbf{D}_{11}(N+1,:) \quad -I_{23}\mathbf{I}(N+1,:)\\ &\frac{I_{24}}{h}\mathbf{I}(N+1,:) \quad \frac{I_{25}}{h}\mathbf{I}(N+1,:)\Big]\mathbf{U}\end{aligned}, \tag{27}$$

$$\begin{bmatrix}-C_{12}\frac{2h}{L}\mathbf{D}_1(N+1,:) & -C_{22}\frac{4h}{L^2}\mathbf{D}_{12}(N+1,:) & C_{23}\frac{2}{L}\mathbf{D}_1(N+1,:)\\ -C_{24}\frac{2}{Lh}\mathbf{D}_1(N+1,:) & -C_{25}\frac{2}{Lh}\mathbf{D}_1(N+1,:)\end{bmatrix}\mathbf{U}=0, \tag{28}$$

$$\begin{bmatrix}C_{13}\frac{2h}{L}\mathbf{D}_1(N+1,:) & -C_{23}\frac{4h}{L^2}\mathbf{D}_{12}(N+1,:) & C_{33}\frac{2}{L}\mathbf{D}_1(N+1,:)\\ -C_{34}\frac{2}{Lh}\mathbf{D}_1(N+1,:) & -C_{35}\frac{2}{Lh}\mathbf{D}_1(N+1,:)\end{bmatrix}\mathbf{U}=0, \tag{29}$$

$$\begin{bmatrix}-C_{14}\frac{2h}{L}\mathbf{D}_1(N+1,:) & C_{24}\frac{4h}{L^2}\mathbf{D}_{12}(N+1,:) & -C_{34}\frac{2}{L}\mathbf{D}_1(N+1,:)\\ C_{44}\frac{2}{Lh}\mathbf{D}_1(N+1,:) & \mathbf{0}(N+1,:)\end{bmatrix}\mathbf{U}=0, \tag{30}$$

$$\begin{bmatrix}C_{15}\frac{2h}{L}\mathbf{D}_1(N+1,:) & C_{25}\frac{4h}{L^2}\mathbf{D}_{12}(N+1,:) & -C_{35}\frac{2}{L}\mathbf{D}_1(N+1,:)\\ \mathbf{0}(N+1,:) & C_{55}\frac{2}{Lh}\mathbf{D}_1(N+1,:)\end{bmatrix}\mathbf{U}=0. \tag{31}$$

The conditions at $x=L$ are expressed as

$$\begin{bmatrix}C_{11}\frac{2h}{L}\mathbf{D}_1(1,:) & C_{12}\frac{4h}{L^2}\mathbf{D}_{12}(1,:) & C_{13}\frac{2}{L}\mathbf{D}_1(1,:)\\ -C_{14}\frac{2}{Lh}\mathbf{D}_1(1,:) & C_{15}\frac{2}{Lh}\mathbf{D}_1(1,:)\end{bmatrix}\mathbf{U}=0, \tag{32}$$

$$\begin{aligned}&\Big[-C_{12}\frac{4h}{L^2}\mathbf{D}_2(1,:) \quad -C_{22}\frac{8h}{L^3}\mathbf{D}_{13}(1,:) \quad C_{23}\frac{4}{L^2}\mathbf{D}_2(1,:)\\ &-C_{24}\frac{4}{L^2h}\mathbf{D}_2(1,:) \quad -C_{25}\frac{4}{L^2h}\mathbf{D}_2(1,:)\Big]\mathbf{U}=\\ &\omega^2\Big[I_{12}h\mathbf{I}(1,:) \quad -I_{22}\frac{2h}{L}\mathbf{D}_{11}(1,:) \quad -I_{23}\mathbf{I}(1,:)\\ &\frac{I_{24}}{h}\mathbf{I}(1,:) \quad \frac{I_{25}}{h}\mathbf{I}(1,:)\Big]\mathbf{U}\end{aligned}, \tag{33}$$

$$\begin{bmatrix}-C_{12}\frac{2h}{L}\mathbf{D}_1(1,:) & -C_{22}\frac{4h}{L^2}\mathbf{D}_{12}(1,:) & C_{23}\frac{2}{L}\mathbf{D}_1(1,:)\\ -C_{24}\frac{2}{Lh}\mathbf{D}_1(1,:) & -C_{25}\frac{2}{Lh}\mathbf{D}_1(1,:)\end{bmatrix}\mathbf{U}=0, \tag{34}$$

$$\begin{bmatrix}C_{13}\frac{2h}{L}\mathbf{D}_1(1,:) & -C_{23}\frac{4h}{L^2}\mathbf{D}_{12}(1,:) & C_{33}\frac{2}{L}\mathbf{D}_1(1,:)\\ -C_{34}\frac{2}{Lh}\mathbf{D}_1(1,:) & -C_{35}\frac{2}{Lh}\mathbf{D}_1(1,:)\end{bmatrix}\mathbf{U}=0, \tag{35}$$

$$\begin{bmatrix}-C_{14}\frac{2h}{L}\mathbf{D}_1(1,:) & C_{24}\frac{4h}{L^2}\mathbf{D}_{12}(1,:) & -C_{34}\frac{2}{L}\mathbf{D}_1(1,:)\\ C_{44}\frac{2}{Lh}\mathbf{D}_1(1,:) & \mathbf{0}(1,:)\end{bmatrix}\mathbf{U}=0, \tag{36}$$

$$\begin{bmatrix}C_{15}\frac{2h}{L}\mathbf{D}_1(1,:) & C_{25}\frac{4h}{L^2}\mathbf{D}_{12}(1,:) & -C_{35}\frac{2}{L}\mathbf{D}_1(1,:)\\ \mathbf{0}(1,:) & C_{55}\frac{2}{Lh}\mathbf{D}_1(1,:)\end{bmatrix}\mathbf{U}=0. \tag{37}$$

Then, the first and $(N+1)$th rows of Eq. (25) should be replaced by Eqs (32) and (26). Similarly, the $(2N+7)$th and $(3N+7)$th rows of Eq. (25) should be replaced by Eqs. (35) and (29). The $(3N+8)$th and $(4N+8)$th rows of Eq. (25) should be replaced by Eqs. (36) and (30). The $(4N+9)$th and $(5N+9)$th rows of Eq. (25) should be replaced by Eqs. (37) and (31). In regard to the variable $\overline{w}_0$, Eqs. (27), (28), (33) and (34) are added into the rows of Eq. (25). The $5N+9$ equations of the standard eigenvalue problem are obtained.

$$\mathbf{L}\mathbf{U}=\omega^2\mathbf{R}\mathbf{U}, \tag{38}$$

where the sizes of matrix $\mathbf{L}$ and $\mathbf{R}$ are $(5N+9)\times(5N+9)$. The iterative procedure [53] is utilized to handle the complex eigenvalue problem considering the frequency-dependent material properties. In this paper, only the examples of cantilevered and free-free beams are presented. The modified spectral collocation method can handle various boundary conditions, such as simply supported, elastically restrained, free end with mass, and so on.

4. Experiment

4.1. Measurement of material properties

For calculating the sandwich beams' resonant frequencies and damping ratios, the master curve of the viscoelastic material is obtained first. The structural adhesive classified as a second-generation acrylic (SGA) adhesive (HARDLOC, C-355–20, Denka) is used to make the specimen. The adhesive is comprised of acrylic resins and acrylic olygomer (rubber), for strength and tenacity. The adhesive is with high viscosity thus, it can be used for vibration reduction. Poisson's ratio is assumed to be real and constant. To measure the Poisson's ratio, the tensile test machine (AGS-10 kN, Shimadzu Corporation) is used with the tensile speed 1 mm/min. The tensile specimen according to JIS K6251–3 (Fig. 3) is cured using the Polytetrafluoroethylene (PTFE) mold at 60 °C for 120 mins as Fig. 2 shows. The surface of the specimen is painted with white paint. Then, the speckle pattern was painted with black paint (Fig. 3). The images of the specimen are captured during the tensile test. The true tensile strain is measured using Digital Image Correlation (DIC) technique [63]. The Poisson's ratio is calculated from the true strain along the tensile direction and that perpendicular to the tensile direction. The variation of Poisson's ratio with tensile strain is shown in Fig. 4. The converged Poisson's ratio is 0.389. The density of the adhesive is 1110 kg/m^3.

The frequency-dependent loss factor and storage modulus are measured using the Oberst beam method [53] [64],. The adhesive is cured on the top surface of the aluminum beam to make the composite beams. Three composite beams are made. The length is 150 mm, and the width is 10 mm. The thickness of the aluminum beam is 1.46 mm. The thicknesses of the specimens' adhesive layers are 1.099, 1.044, and 0.937 mm, respectively. The cantilevered specimens are clamped by the fixture. The vibration of the specimen is excited by a steel ball. The steel ball is stuck by an electromagnet, and then it dropped freely to the surface of the aluminum beam. The velocity history of a point is measured by a laser Doppler vibrometer (VibroGo, Polytec). The experimental setup is shown in Fig. 5. The sampling frequency and time are 50 kHz and 2 s, respectively. All the experiments are conducted at room temperature (20°C). The natural frequencies of specimen are obtained by choosing local peaks from fast Fourier transform (FFT) results

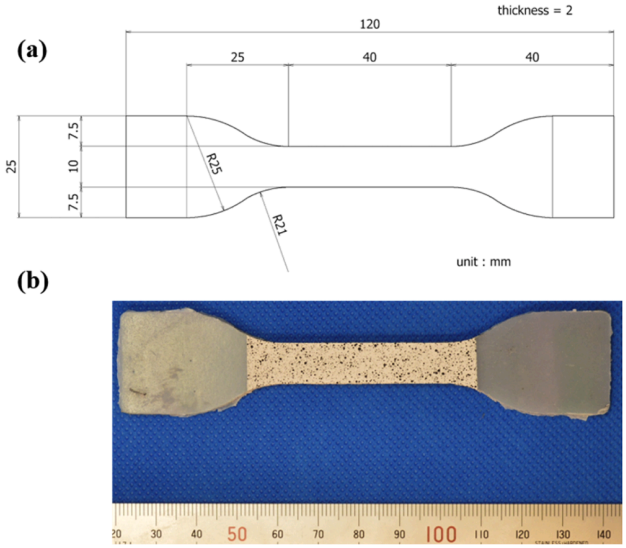

Fig. 3. (a) Configure of bulk specimen (b) Photo of bulk specimen.

of the measured velocity history. Then, the impulse response function (IRF) of each mode is obtained by applying a band-pass filter to the original data. The damping factor ξ_c at the natural frequency can be determined through fitting an exponential decay function to the IRF [53] [65],. Then, the loss factors η_c is obtained $\eta_c = 2\xi_c\sqrt{1-\xi_c^2}$. Fig. 6 (a) shows an example of original and filtered power spectral density (PSD) functions. Fig. 6(b) shows an example of original and fitting IRF. The measured frequency-dependent storage modulus and loss factor of SGA are shown in Fig. 7. The fitting storage modulus and loss factor are expressed as

$$E_c(f) = -2\times10^{-9}f^2 + 1.77\times10^{-5}f + 2.296[\text{GPa}] \tag{39}$$

$$\eta_c(f) = 1.05\times10^{7}e^{-\left((f-9.334\times10^5)/2.138\times10^5\right)^2} + 0.04924e^{-((f-804.8)/729.2)^2} \tag{40}$$

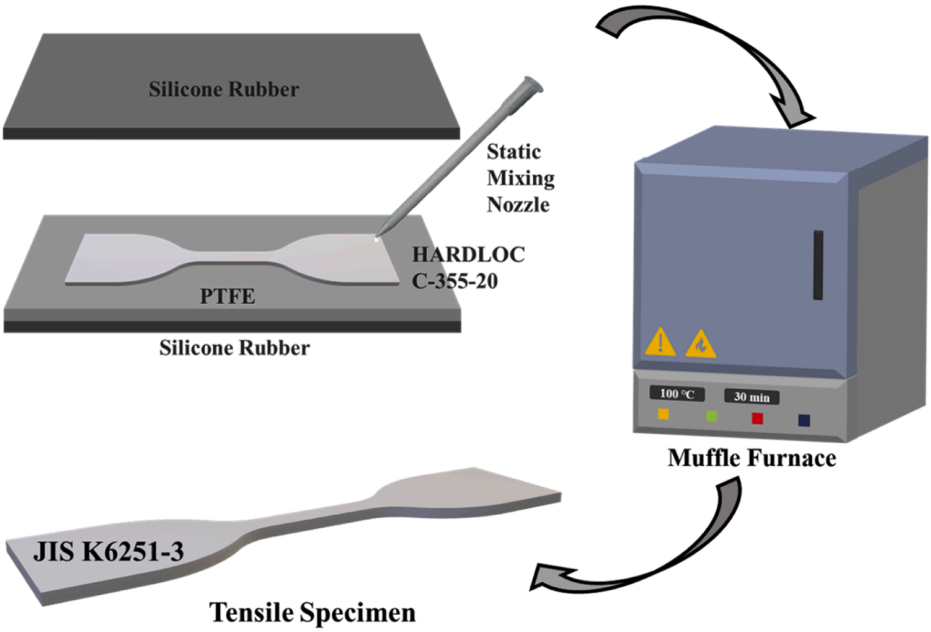

Fig. 2. Schematic of making tensile test specimen.

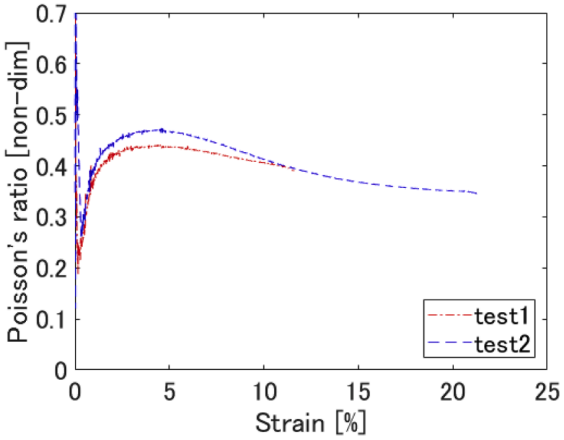

Fig. 4. Measured Poisson's ratio.

4.2. Experiments of sandwich beams

Experiments with two different boundary conditions: free-free and clamped-free are conducted. The specimens are made of aluminum beams (A6061-T6) bounded by SGA (HARDLOC, C-355–20, Denka). The adhesive is cured at 60 °C for 120 mins. Four specimens are made for the experiments with free-free boundary conditions. The thicknesses of the four specimens are listed in Table 1. The specimens' length and width are 200 and 25 mm. The sandwich beam is placed on two rubbers to simulate the free-free boundary conditions. The mallet is used to hit the specimen. A bridge (SB 102 B, Tokyo Measuring Instruments Laboratory Co., Ltd.), a strain gauge (FLA-2–11, Tokyo Measuring Instruments Laboratory Co., Ltd.), and a DC strain amplifier (AS2101, NEC San-ei Instruments, Ltd.) are utilized to record the strain history as Fig. 8 shows. The strain gauge is attached at the center of the beam. The sandwich beams' natural frequencies and loss factors were determined using the same data analysis method presented in Section 4.1. Three specimens are made for the experiments with clamped-free boundary conditions. In Table 2, the thicknesses of specimens are provided. The specimens' length and width are 160 and 10 mm. The specimens are clamped by the fixture. The specimens are struck by a steel ball near the fixture. The velocity history of a point is measured by a laser Doppler vibrometer (VibroGo, Polytec) as Fig. 9 shows. The measurement location is 60 mm far away from the free end.

5. Results and discussion

5.1. Convergence test

The convergence test of the proposed method was investigated by comparing the calculated natural frequencies and loss factors with the published experimental results [66]. The thickness of the sandwich beam is defined as $h^t - h^c - h^b$ mm, where h^t is the thickness of the top layer, h^c is the thickness of the core, and h^b is the thickness of the bottom layer. In this case, the thickness of the sandwich beam is 1–1–1 mm. The length and width of the cantilevered sandwich beam are 475 mm and 30 mm. The viscoelastic core is Polyurethane dielectric resin: RE 12,461 Polyol – RE 1010 Isocyanate, which is sandwiched by two aluminum beams. The Poisson's ratio and density of the viscoelastic layer are 0.3 and 1500 kg/m^3. The Young's modulus, Poisson's ratio, and density of the aluminum are 70 GPa, 0.33, and 2700 kg/m^3, respectively. The core's shear modulus G^* and loss factor η are

$$G^* = 10^6 + 2.9907 \times 10^4\omega + 0.637\omega^2[\text{Pa}], \tag{41}$$

$$\eta = -0.1912 - \frac{50.2153}{\omega} + \frac{3.2341}{\omega^2}. \tag{42}$$

The modified spectral collocation method (MSCM) convergence test of the first seventh natural frequencies and loss factors for the sandwich beam is presented in Table 3. When N= 16, the results have converged. Table 4 shows the convergence test of first seventh natural frequencies

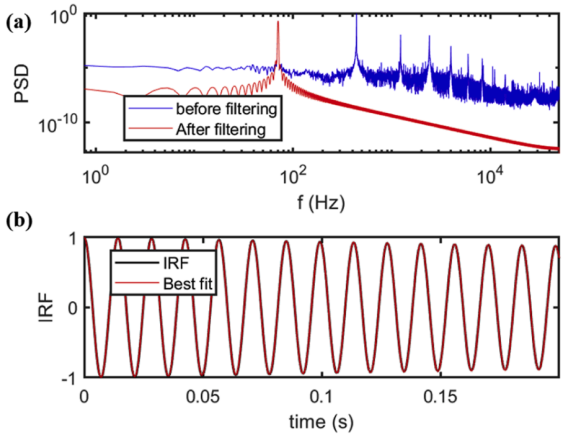

Fig. 6. An example of (a) original and filtered PSD (b) original and fitting IRF.

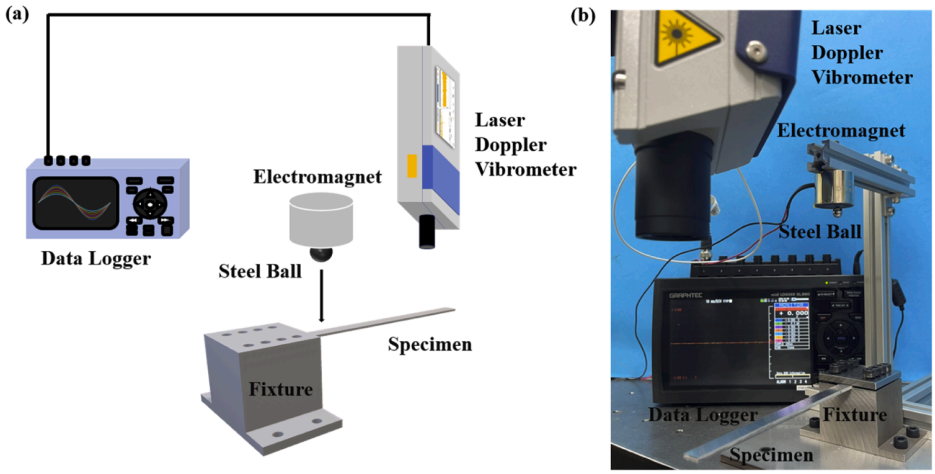

Fig. 5. (a) Schematic of experimental setup for measuring storage modulus and loss factor of adhesive (b) Photo of experimental setup.

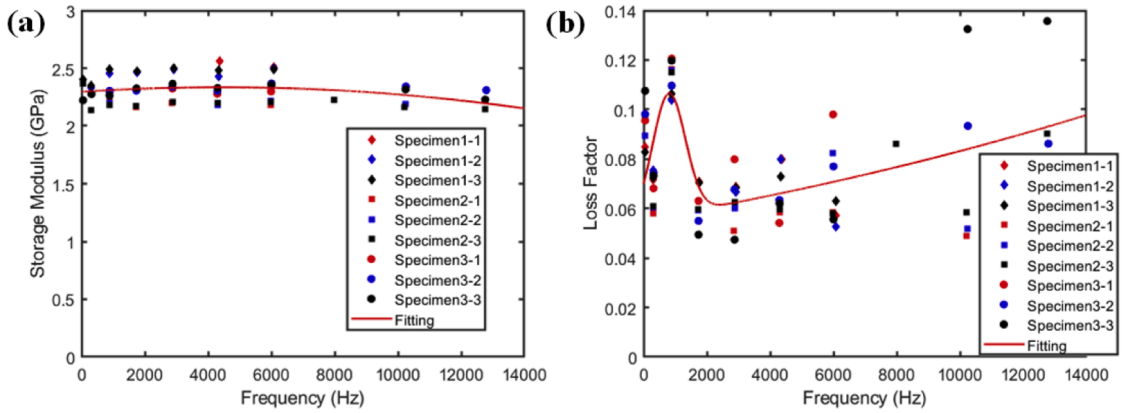

Fig. 7. (a) Frequency-dependent storage modulus (b) Frequency-dependent loss factor.

Table 1
Thicknesses of specimens with free-free boundary conditions.

	Top [mm]	Core [mm]	Bottom [mm]
Specimen 1	1	0.421	1
Specimen 2	1	0.991	1
Specimen 3	1	0.393	1.5
Specimen 4	1	0.952	1.5

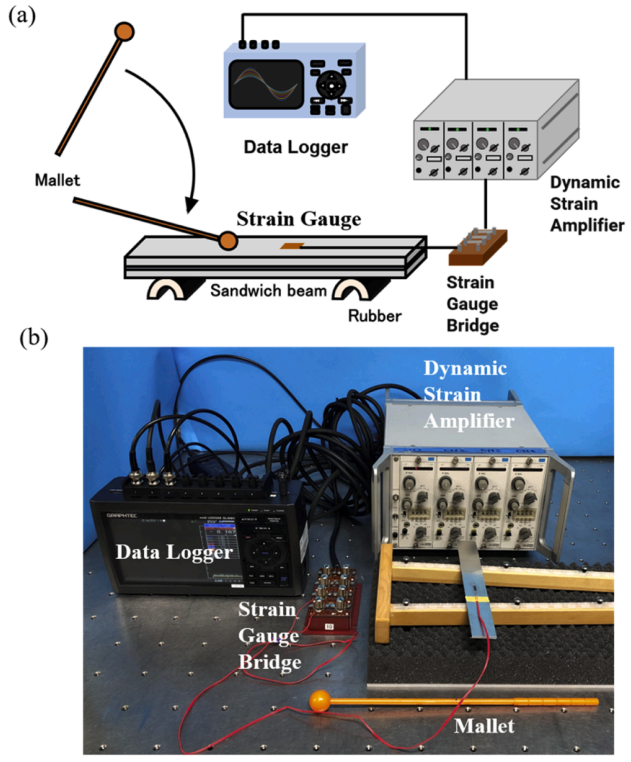

Fig. 8. (a) Schematic of experimental setup for free-free sandwich beams (b) Photo of experimental setup.

and loss factors using conventional spectral collocation method. It shows that there are some differences between the results obtained using conventional spectral collocation method and experimental results and those obtained using FEM [67] and modified spectral collocation method. In the following calculations, the point number N= 20 is used.

Table 2
Thicknesses of specimens with clamped-free boundary conditions.

	Top [mm]	Core [mm]	Bottom [mm]
Specimen 1	0.47	0.701	0.93
Specimen 2	0.47	0.903	0.93
Specimen 3	0.47	1.265	0.93

5.2. Validation

To validate the modified spectral collocation method, the numerical studies of sandwich beams containing viscoelastic cores with constant viscoelastic model and frequency dependent viscoelastic model are conducted [68]. The length and width of the cantilevered sandwich beam are 177.8 mm and 12.7 mm. The sandwich beam's thcikness is 1.524–0.127–1.524 mm. The used Young's modulus, Poisson's ratio, and density of the aluminum are 69 GPa, 0.3, and 2766 kg/m^3, respectively. The Young's modulus, Poisson's ratio, and density of the viscoelastic core are 1.794 MPa, 0.3, and 968.1 kg/m^3, respectively. The different constant loss factors η_c are used. Table 5 shows the first six modes' natural frequencies f and loss factor's ratios η/η_c of cantilevered beams for various core's loss factors. The MSCM means the modified spectral collocation method. The RM is the real eigenmodes. The ACM is the approached complex eigenmodes [68]. The results in Bilasse et al.'s paper [69] are obtained by using diamant approach, a generic and efficient automatic differentiation implementation of asymptotic numerical method (ANM). The results in Abdoun et al.'s paper [70] are obtained by performing the forced harmonic vibration using an asymptotic numerical method. The results obtained using MSCM are in excellent agreement with ACM [68] and Bilasse et al.'s results [69]. As stated in the reference [68], RM underestimates the natural frequencies and overestimates the loss factors for large core's loss factors. MSCM based on a higher-order layer-wise beam theory can exactly estimate the loss factors and resonant frequencies of cantilevered sandwich beams. Then, the numerical results for frequency dependent materials are compared. The 3 M ISD112 is used first [68]. The complex shear modulus of 3 M ISD112 is expressed as [68,71,72]

$$G^c(\omega) = G_0\left(1 + \sum_{k=1}^{3} \frac{\Delta_k \omega}{\omega - \mathrm{i}\Omega_k}\right) \tag{43}$$

where the fitting parameters at 20 and 27 °C are shown in Table 6. The density and Poisson's ratio of 3 M ISD112 are 1600 kg/m^3 and 0.5, respectively. Then, Polyvinyl-Butyral (PVB) is used. The complex shear modulus of PVB is expressed as [73]

$$G^c(\omega) = G_\infty + (G_0 - G_\infty)\left[1 + (\mathrm{i}\omega\tau)^{1-\alpha}\right]^{-\beta} \tag{44}$$

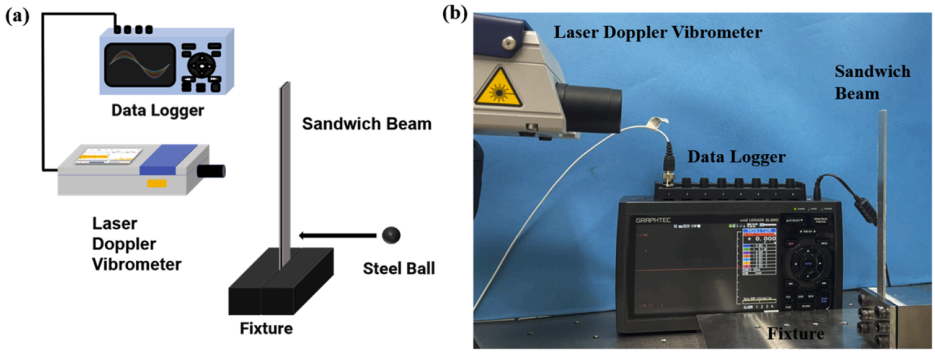

Fig. 9. (a) Schematic of experimental setup for clamped-free sandwich beams (b) Photo of experimental setup.

Table 3
Convergence of results using modified spectral collocation method.

Mode		1	2	3	4	5	6	7
Experiment [66]	Frequency [Hz]	10.79	67.18	186.74	363.98	598.15	885.37	1214.99
	Loss factor	0.061	0.070	0.082	0.041	0.041	0.049	0.015
FEM [67]	Frequency [Hz]	10.43	62.99	177.76	349.27	579.29	868.59	1218.10
	Loss factor	0.027	0.083	0.063	0.050	0.040	0.032	0.026
N= 10	Frequency [Hz]	10.43	62.92	177.61	349.02	580.95	864.69	1415.05
	Loss factor	0.027	0.083	0.063	0.050	0.040	0.031	0.026
N= 12	Frequency [Hz]	10.43	62.92	177.64	349.05	578.99	867.77	1240.71
	Loss factor	0.027	0.083	0.063	0.050	0.040	0.033	0.026
N= 14	Frequency [Hz]	10.43	62.92	177.66	349.09	579.05	868.31	1218.61
	Loss factor	0.027	0.083	0.063	0.050	0.040	0.033	0.027
N= 16	Frequency [Hz]	10.43	62.92	177.66	349.11	579.08	868.35	1217.88
	Loss factor	0.027	0.083	0.063	0.050	0.040	0.033	0.026
N= 18	Frequency [Hz]	10.43	62.92	177.66	349.11	579.11	868.39	1217.86
	Loss factor	0.027	0.083	0.063	0.050	0.040	0.033	0.026
N= 20	Frequency [Hz]	10.43	62.92	177.66	349.12	579.12	868.41	1217.90
	Loss factor	0.027	0.083	0.063	0.050	0.040	0.033	0.026

Table 4
Convergence of results using conventional spectral collocation method.

Mode		1	2	3		5	6	7
N= 16	Frequency [Hz]	10.92	65.97	186.56	364.94	608.39	906.17	1280.48
	Loss factor	0.029	0.079	0.060	0.046	0.038	0.030	0.024
N= 18	Frequency [Hz]	10.92	65.97	186.56	364.94	608.39	906.17	1280.48
	Loss factor	0.029	0.079	0.060	0.046	0.038	0.030	0.024
N= 20	Frequency [Hz]	10.92	65.97	186.56	364.94	608.39	906.17	1280.48
	Loss factor	0.029	0.079	0.060	0.046	0.038	0.030	0.024

where $G_0 = 0.479$ MPa, $G_\infty = 0.235$ GPa, $\tau = 0.3979$, $\alpha = 0.46$, and $\beta = 0.1946$. The density and Poisson's ratio of PVB are 999 kg/m^3 and 0.4, respectively. Table 7 shows the results of the first four modes of cantilevered sandwich beams with various frequency-dependent viscoelastic cores. Table 8 shows results of the first modes of clamped-clamped sandwich beams with various frequency dependent viscoelastic cores. The IRM means improved real eigenmodes. The ECM means exact complex eigenmodes, in which ANM is used to solve the eigenvalue problem without any approximation. The details of the different methods are in Bilasse et al.'s paper [68]. The MSCM can get closer results compared with ACM and ECM for different frequency dependent viscoelastic materials. The RM is not suitable to estimate the natural frequencies and loss factors of sandwich beams with PVB core. Above all, the MSCM based on a higher-order layer-wise beam theory is accurate and efficient to estimate the sandwich beams' resonant frequencies and loss factors with various viscoelastic cores and various boundary conditions.

5.3. Experimental results and discussion

In the theoretical calculations, the Young's modulus, Poisson's ration and density of aluminum are 70 GPa, 0.33, 2711 kg/m^3, respectively. Table 9 shows the experimental and theoretical natural frequencies and loss factors of first five modes for free-free sandwich beams. The present theory can predict the natural frequencies of symmetric (Specimens 1 and 2) and asymmetric (Specimens 3 and 4) sandwich beams accurately. The difference between theoretical and experimental results increases as the natural frequency increases. The present theory can predict the loss factors accurately for low modes. However, there are large differences between experimental and theoretical loss factors for high modes, especially for asymmetric sandwich beams. It is because that large variations of loss factors exist for high frequency as Fig. 7(b) shows. Table 10 shows the experimental and theoretical natural frequencies and loss factors of first five modes for clamped-free sandwich beams. The present theory can predict the natural frequency and loss factor for clamped-free sandwich beams accurately. The thickness of the core of the three specimens are 0.701, 0.903, and 1.265 mm. The experimental natural frequencies of the three specimens' fifth mode are 3640.4,

Table 5
Natural frequencies and loss factors of cantilevered sandwich beams for different core's loss factors.

η_c	MSCM		RM [68]		ACM [68]		Bilasse et al. [69]		Abdoun et al. [70]	
	f [Hz]	η/η_c	f [Hz]	η/η_c	f [Hz]	η/η_c	f [Hz]	η/η_c	f [Hz]	η/η_c
0.1	64.1	0.281	64.1	0.283	64.1	0.281	64.1	0.281	64.5	0.281
	296.5	0.242	296.6	0.243	296.6	0.242	296.7	0.242	298.9	0.242
	743.5	0.154	744.3	0.154	744.4	0.154	744.5	0.154	746.5	0.154
	1392.5	0.089	1395.2	0.089	1395.6	0.088	1395.7	0.089	1407.7	0.089
	2256.4	0.057	2263.4	0.057	2264.5	0.057	2264.5	0.057	2286.2	0.057
	3332.2	0.039	3347.3	0.039	3349.5	0.039	3349.8	0.039	3385.7	0.039
0.6	65.5	0.246	64.1	0.283	65.5	0.246	65.5	0.246	65.9	0.247
	299.0	0.232	296.6	0.243	299.1	0.232	299.2	0.232	303.1	0.224
	745.3	0.152	744.3	0.154	746.2	0.152	746.3	0.153	752.3	0.150
	1393.5	0.088	1395.2	0.089	1396.6	0.088	1396.6	0.089	1412.7	0.088
	2257.0	0.057	2263.4	0.057	2265.1	0.057	2265.2	0.057	2290.6	0.057
	3332.6	0.039	3347.3	0.039	3350.1	0.038	3350.2	0.039	3389.5	0.039
1	67.5	0.202	64.1	0.283	67.4	0.202	67.5	0.202	67.8	0.204
	302.9	0.217	296.6	0.243	303.0	0.217	303.1	0.218	309.1	0.201
	748.5	0.150	744.3	0.154	749.4	0.150	749.4	0.150	761.1	0.142
	1395.1	0.088	1395.2	0.089	1397.9	0.088	1398.3	0.088	1420.6	0.086
	2258.2	0.057	2263.4	0.057	2266.3	0.057	2266.3	0.057	2297.9	0.057
	3333.4	0.039	3347.3	0.039	3350.9	0.038	3350.9	0.039	3395.9	0.037
1.5	69.9	0.153	64.1	0.283	69.9	0.153	69.9	0.153	70.3	0.155
	308.9	0.197	296.6	0.243	309.1	0.197	309.1	0.198	317.4	0.176
	754.3	0.146	744.3	0.154	755.2	0.145	755.2	0.146	777.2	0.131
	1398.2	0.087	1395.2	0.089	1401.4	0.087	1401.4	0.087	1432.8	0.083
	2260.3	0.057	2263.4	0.057	2268.4	0.056	2268.5	0.057	2310.1	0.056
	3334.8	0.039	3347.3	0.039	3352.3	0.038	3352.3	0.039	3307.0	0.039

Table 6
Material parameters of 3 M ISD 112 at 20 and 27 °C [68,71,72].

k	20 °C			27 °C		
	G_0 [Pa]	Δ_k	Ω_k [rad/s]	G_0 [Pa]	Δ_k	Ω_k [rad/s]
1	0.0511E6	2.8164	31.1176	0.5E6	0.746	468.7
2		13.1162	446.4542		3.265	4742.4
3		45.4655	5502.5318		43.284	71,532.5

3998.2, and 4421.6 Hz. The experimental loss factors of the three specimens' fifth mode are 0.0094, 0.0136, and 0.0212. It can conclude that as the thickness of the core increases, the natural frequencies and loss factors increase. Moreover, the difference between the theoretical and experimental results increases, as the thickness and natural frequency increase. Generally, the present theory can predict natural frequences and loss factors of symmetric or asymmetric sandwich beams with thin or thick viscoelastic cores. Up until now, only sandwich beams with stiff faces and soft cores have been discussed. The problem of hard cores still needs further discussion.

6. Conclusions

In the paper, vibration characteristics of sandwich beams containing a viscoelastic core with different boundary conditions were investigated. A higher-order layer-wise beam theory was presented to describe the displacement field of the sandwich beams with viscoelastic cores. The Hamilton's principle was used to derive the equations of motion and boundary conditions. A modified spectral collocation method was used to solve the equations of motion with different boundary conditions by combining the integrated-based spectral collocation method and conventional spectral collocation method, which can implement multiple boundary conditions at one boundary point. The present theory was accurate and efficient to estimate the loss factors and resonant frequencies of sandwich beams containing viscoelastic cores with constant viscoelastic model and frequency dependent viscoelastic model. Moreover, the present theory can predict natural frequences and loss factors of symmetric or asymmetric sandwich beams with thin or thick viscoelastic cores and different boundary conditions. The present method is also accurate when the thickness of the core to that of the sandwich beam equals 0.475.

It was found that the storage modulus and loss factor of the adhesive

Table 7
Natural frequencies and loss factors of cantilevered sandwich beams for frequency dependent core materials.

MSCM		RM [68]		IRM [68]		ACM [68]		ECM [68]	
f [Hz]	η	f [Hz]	η	f [Hz]	η	f [Hz]	η	f [Hz]	η
3 M ISD112 core at 20 °C									
64.27	2.28E-01	65.97	7.32E-01	58.31	3.61E-01	61.96	2.62E-01	63.07	1.96E-01
319.87	2.04E-01	340.04	3.98E-01	309.04	2.16E-01	314.58	1.98E-01	316.54	1.87E-01
833.68	1.59E-01	845.85	2.51E-01	813.76	1.75E-01	821.85	1.69E-01	823.29	1.60E-01
1535.75	8.76E-02	1562.42	1.26E-01	1526.99	9.71E-02	1530.85	9.63E-02	1530.60	9.48E-02
3 M ISD112 core at 27 °C									
65.31	1.60E-01	63.74	2.39E-01	63.38	1.86E-01	65.04	1.59E-01	65.34	1.56E-01
325.95	2.71E-01	317.33	4.06E-01	312.34	3.02E-01	322.47	2.60E-01	326.08	2.55E-01
851.37	2.96E-01	827.62	4.19E-01	814.19	3.25E-01	839.97	2.88E-01	849.49	2.78E-01
1568.70	2.83E-01	1540.09	3.52E-01	1523.79	2.91E-01	1556.38	2.70E-01	1567.53	2.69E-01
PVB core at 20 °C									
81.79	1.34E-03	488.78	2.12E-01	81.78	1.54E-03	81.80	1.48E-03	81.79	1.37E-03
503.83	5.12E-03	2082.08	1.55E-01	503.95	6.12E-03	504.17	5.98E-03	504.16	5.43E-03
1377.89	8.71E-03	4183.69	1.29E-01	1379.56	1.04E-02	1380.38	1.02E-02	1380.34	9.38E-03
2618.56	1.25E-02	6090.64	1.13E-01	2626.08	1.48E-02	2627.92	1.46E-02	2627.87	1.36E-02

Table 8
Natural frequencies and loss factors of clamped-clamped sandwich beams for frequency dependent core materials.

MSCM		RM [68]		IRM [68]		ACM [68]		ECM [68]	
f [Hz]	η	f [Hz]	η	f [Hz]	η	f [Hz]	η	f [Hz]	η
3 M ISD112 core at 20 °C									
289.86	1.90E-01	289.24	2.28E-01	285.06	1.88E-01	287.38	1.83E-01	288.07	1.80E-01
779.33	1.36E-01	781.95	1.77E-01	769.52	1.42E-01	773.39	1.39E-01	774.05	1.36E-01
1484.39	7.62E-02	1494.62	9.70E-02	1480.16	8.21E-02	1482.51	8.17E-02	1482.42	8.09E-02
2379.85	4.01E-02	2398.41	4.88E-02	2385.10	4.31E-02	2386.03	4.31E-02	2385.94	4.30E-02
3 M ISD112 core at 27 °C									
293.02	2.58E-01	288.11	2.91E-01	286.88	2.59E-01	291.38	2.47E-01	292.70	2.49E-01
786.36	2.55E-01	774.38	3.05E-01	768.85	2.61E-01	781.34	2.46E-01	784.94	2.45E-01
1502.56	2.43E-01	1485.64	2.79E-01	1476.96	2.44E-01	1492.02	2.34E-01	1502.34	2.34E-01
2434.31	2.36E-01	2412.39	2.62E-01	2401.45	2.34E-01	2428.93	2.26E-01	2436.94	2.27E-01
PVB core at 20 °C									
504.34	7.53E-03	1631.84	1.56E-01	506.46	9.14E-03	506.79	8.94E-03	506.77	8.03E-03
1350.34	1.16E-02	3382.00	1.28E-01	1357.71	1.38E-02	1358.75	1.36E-02	1358.71	1.25E-02
2560.52	1.52E-02	5280.18	1.11E-01	2579.46	1.79E-02	2571.56	1.77E-02	2581.50	1.65E-02
4080.60	1.83E-02	7241.05	9.88E-02	4120.84	2.14E-02	4124.21	2.12E-02	4124.14	2.00E-02

Table 9
Comparison between experimental and theoretical results for free-free sandwich beams.

Specimen 1				Specimen 2			
Theoretical		Experimental		Theoretical		Experimental	
f [Hz]	η	f [Hz]	η	f [Hz]	η	f [Hz]	η
332.0	0.0028	329.2	0.0022	425.0	0.0023	427.6	0.0028
908.8	0.0039	917.1	0.0059	1152.5	0.0036	1154.3	0.0046
1762.4	0.0039	1779.6	0.0096	2204.4	0.0036	2210.2	0.0061
2872.7	0.0033	2908.7	0.0138	3532.4	0.0036	3546.5	0.0109
4218.8	0.0037	4131.3	0.0187	5088.0	0.0940	5127.3	0.0115
Specimen 3				Specimen 4			
Theoretical		Experimental		Theoretical		Experimental	
f [Hz]	η	f [Hz]	η	f [Hz]	η	f [Hz]	η
389.5	0.0037	394.4	0.0026	478.4	0.0033	480.3	0.0025
1065.5	0.0040	1076.1	0.0030	1294.7	0.0036	1300.0	0.0090
2064.1	0.0821	2092.4	0.0028	2470.0	0.0035	2487.2	0.0087
3360.0	0.0794	3353.1	0.0061	3946.5	0.0793	4005.8	0.0084
4927.1	0.0795	5030.1	0.0075	5667.4	0.0712	5701.4	0.0072

Table 10
Comparison between experimental and theoretical results for clamped-free sandwich beams.

	Theoretical		Experimental	
	f [Hz]	η	f [Hz]	η
Specimen 1	71.0	0.0035	69.4	0.0059
	441.2	0.0070	428.4	0.0040
	1218.4	0.0118	1172.6	0.0066
	2340.8	0.0129	2255.2	0.0128
	3778.1	0.0181	3640.4	0.0094
Specimen 2	78.3	0.0038	78.2	0.0049
	485.3	0.0085	479.1	0.0041
	1334.5	0.0137	1314.2	0.0073
	2549.7	0.0157	2494.4	0.0254
	4089.0	0.0224	3998.2	0.0136
Specimen 3	91.0	0.0043	95.4	0.0042
	560.8	0.0112	552.7	0.0050
	1530.5	0.0163	1493.5	0.0077
	2896.3	0.0206	2822.9	0.0346
	4595.0	0.0296	4421.6	0.0212

varied greatly for high frequency. Thus, the uncertainties of the adhesive's frequency-dependent storage modulus and loss factor can be further considered in the present theory [74,75]. Besides, the present method can be extended to solve the problem of sandwich laminated beams.

CRediT authorship contribution statement

Ming Ji: Writing – review & editing, Writing – original draft, Visualization, Validation, Software, Methodology, Investigation, Data curation. **Yu Sekiguchi:** Writing – review & editing, Investigation, Conceptualization. **Masanobu Naito:** Writing – review & editing, Project administration, Funding acquisition. **Chiaki Sato:** Writing – review & editing, Supervision, Project administration, Funding acquisition, Conceptualization.

Declaration of competing interest

The authors declare that they have no known competing financial interests or personal relationships that could have appeared to influence the work reported in this paper.

Acknowledgements

The authors would like to thank Mr. Sugihara at Design and Manufacturing Division, Open Facility Center, Tokyo Institute of Technology, for preparing the fixture. The authors would like to thank Mr. Onodera at Department of Mechanical Engineering, Tokyo Institute of Technology, for helping to measure the material properties of adhesive.

This work was supported by the Core Research for Evolutional Science and Technology (CREST) program "Revolution material development by fusion of strong experiments with theory/data science" of the

Japan Science and Technology Agency (JST), Japan [grant number: JPMJCR19J3].

Appendix

The variables of force and moment terms in Eqs. (11) through (15) can be expressed as

$$
\begin{aligned}
&N_x^t=\int_{h^c/2}^{h^c/2+h^t}\sigma_x^t\mathrm{d}z, N_x^c=\int_{-h^c/2}^{h^c/2}\sigma_x^c\mathrm{d}z, N_x^b=\int_{-h^c/2-h^b}^{-h^c/2}\sigma_x^b\mathrm{d}z,\\
&M_x^t=\int_{h^c/2}^{h^c/2+h^t}z\sigma_x^t\mathrm{d}z, M_x^c=\int_{-h^c/2}^{h^c/2}z\sigma_x^c\mathrm{d}z, M_x^b=\int_{-h^c/2-h^b}^{-h^c/2}z\sigma_x^b\mathrm{d}z,\\
&P_x^t=\int_{h^c/2}^{h^c/2+h^t}l(z)\sigma_x^t\mathrm{d}z, P_x^b=\int_{-h^c/2-h^b}^{-h^c/2}l(z)\sigma_x^b\mathrm{d}z,\\
&Q_x^t=\int_{h^c/2}^{h^c/2+h^t}m(z)\sigma_x^t\mathrm{d}z, Q_x^b=\int_{-h^c/2-h^b}^{-h^c/2}n(z)\sigma_x^b\mathrm{d}z,\\
&R_{xz}^t=\int_{h^c/2}^{h^c/2+h^t}\frac{\partial l(z)}{\partial z}\tau_{xz}^t\mathrm{d}z, R_{xz}^b=\int_{-h^c/2-h^b}^{-h^c/2}\frac{\partial l(z)}{\partial z}\tau_{xz}^b\mathrm{d}z,\\
&R_{xz}^t=\int_{h^c/2}^{h^c/2+h^t}\frac{\partial l(z)}{\partial z}\tau_{xz}^t\mathrm{d}z, R_{xz}^c=\int_{-h^c/2}^{h^c/2}\tau_{xz}^c\mathrm{d}z, R_{xz}^b=\int_{-h^c/2-h^b}^{-h^c/2}\frac{\partial l(z)}{\partial z}\tau_{xz}^b\mathrm{d}z,\\
&S_{xz}^t=\int_{h^c/2}^{h^c/2+h^t}\frac{\partial m(z)}{\partial z}\tau_{xz}^t\mathrm{d}z, S_{xz}^b=\int_{-h^c/2-h^b}^{-h^c/2}\frac{\partial n(z)}{\partial z}\tau_{xz}^b\mathrm{d}z.
\end{aligned}
\tag{A.1}
$$

The parameters of the inertia in Eqs. (11) through (15) are expressed as

$$
\begin{aligned}
&I_{11}=\left(\rho^t h^t+\rho^c h^c+\rho^b h^b\right), I_{12}=-\frac{\rho^t h^t}{2}\left(h^t+h^c\right)+\frac{\rho^b h^b}{2}\left(h^b+h^c\right),\\
&I_{13}=\rho^t h^t\left(\frac{G^c h^t}{3G^t}+\frac{h^c}{2}\right)+\rho^b h^b\left(\frac{G^c h^b}{3G^b}+\frac{h^c}{2}\right), I_{14}=-\frac{\rho^t\left(h^t\right)^3}{12}, I_{15}=\frac{\rho^b\left(h^b\right)^3}{12},\\
&I_{22}=-\left(\frac{\rho^t}{24}\left(\left(2h^t+h^c\right)^3-\left(h^c\right)^3\right)+\frac{\rho^c\left(h^c\right)^3}{12}+\frac{\rho^b h^b}{24}\left(\left(2h^b+h^c\right)^3-\left(h^c\right)^3\right)\right),\\
&I_{23}=\rho^t h^t\left(\frac{G^c h^t\left(5h^t+4h^c\right)}{24G^t}+\frac{h^c\left(h^t+h^c\right)}{4}\right)+\frac{\rho^c\left(h^c\right)^3}{12}\\
&\qquad+\rho^b h^b\left(\frac{G^c h^b\left(5h^b+4h^c\right)}{24G^b}+\frac{h^c\left(h^b+h^c\right)}{4}\right),\\
&I_{24}=-\frac{\rho^t\left(h^t\right)^3\left(7h^t+5h^c\right)}{120}, I_{25}=-\frac{\rho^b\left(h^b\right)^3\left(7h^b+5h^c\right)}{120},\\
&I_{33}=\rho^t h^t\left(\frac{2}{15}\left(\frac{G^c h^t}{G^t}\right)^2+\frac{G^c h^c h^t}{3G^t}+\frac{\left(h^c\right)^2}{4}\right)+\frac{\rho^c\left(h^c\right)^3}{12}\\
&\qquad+\rho^b h^b\left(\frac{2}{15}\left(\frac{G^c h^b}{G^b}\right)^2+\frac{G^c h^c h^b}{3G^b}+\frac{\left(h^c\right)^2}{4}\right),\\
&I_{34}=-\rho^t\left(h^t\right)^3\left(\frac{13G^c h^t}{360G^t}+\frac{h^c}{24}\right), I_{35}=-\rho^b\left(h^b\right)^3\left(\frac{13G^c h^b}{360G^b}+\frac{h^c}{24}\right),
\end{aligned}
\tag{A.2}
\tag{A.3}
\tag{A.4}
$$

$$
I_{44}=\frac{13\rho^t\left(h^t\right)^5}{1260}, I_{55}=\frac{13\rho^b\left(h^b\right)^5}{1260}.
\tag{A.5}
$$

The terms in the matrix in Eq. are expressed as

$$
\begin{aligned}
&\mathbf{L}_{11}=C_{11}\frac{4h}{L^2}\mathbf{D}_2, \mathbf{L}_{12}=C_{12}\frac{8h}{L^3}\mathbf{D}_{\mathrm{I}3}, \mathbf{L}_{13}=C_{13}\frac{4}{L^2}\mathbf{D}_2,\\
&\mathbf{L}_{14}=-C_{14}\frac{4}{L^2h}\mathbf{D}_2, \mathbf{L}_{15}=C_{15}\frac{4}{L^2h}\mathbf{D}_2,
\end{aligned}
\tag{A.6}
$$

$$\mathbf{L}_{21}=C_{12}\frac{8h}{L^3}\mathbf{D}_3,\mathbf{L}_{22}=-C_{22}\frac{16h}{L^4}\mathbf{D}_{14},\mathbf{L}_{23}=C_{23}\frac{8}{L^3}\mathbf{D}_3,$$
$$\mathbf{L}_{24}=-C_{24}\frac{8}{L^3h}\mathbf{D}_3,\mathbf{L}_{25}=-C_{25}\frac{8}{L^3h}\mathbf{D}_3, \tag{A.7}$$

$$\mathbf{L}_{31}=C_{13}\frac{4h}{L^2}\mathbf{D}_2,\mathbf{L}_{32}=-C_{23}\frac{8h}{L^3}\mathbf{D}_{13},\mathbf{L}_{33}=C_{33}\frac{4}{L^2}\mathbf{D}_2-F_{33}\mathbf{I},$$
$$\mathbf{L}_{34}=-C_{34}\frac{4}{L^2h}\mathbf{D}_2+\frac{F_{34}}{h}\mathbf{I},\mathbf{L}_{35}=-C_{35}\frac{4}{L^2h}\mathbf{D}_2+\frac{F_{35}}{h}\mathbf{I}, \tag{A.8}$$

$$\mathbf{L}_{41}=-C_{14}\frac{4h}{L^2}\mathbf{D}_2,\mathbf{L}_{42}=C_{24}\frac{8h}{L^3}\mathbf{D}_{13},\mathbf{L}_{43}=-C_{34}\frac{4}{L^2}\mathbf{D}_2+F_{34}\mathbf{I},$$
$$\mathbf{L}_{44}=C_{44}\frac{4}{L^2h}\mathbf{D}_2-\frac{F_{44}}{h}\mathbf{I},\mathbf{L}_{45}=\mathbf{0}, \tag{A.9}$$

$$\mathbf{L}_{51}=C_{15}\frac{4h}{L^2}\mathbf{D}_2,\mathbf{L}_{52}=C_{25}\frac{8h}{L^3}\mathbf{D}_{13},\mathbf{L}_{53}=-C_{35}\frac{4}{L^2}\mathbf{D}_2+F_{35}\mathbf{I},$$
$$\mathbf{L}_{54}=\mathbf{0},\mathbf{L}_{55}=C_{55}\frac{4}{L^2h}\mathbf{D}_2-\frac{F_{55}}{h}\mathbf{I}, \tag{A.10}$$

$$\mathbf{R}_{11}=-I_{11}h\mathbf{I},\mathbf{R}_{12}=-I_{12}\frac{2h}{L}\mathbf{D}_{11},\mathbf{R}_{13}=-I_{13}\mathbf{I},\mathbf{R}_{14}=-\frac{I_{14}}{h}\mathbf{I},\mathbf{R}_{15}=-\frac{I_{15}}{h}\mathbf{I}, \tag{A.11}$$

$$\mathbf{R}_{21}=-I_{12}\frac{2h}{L}\mathbf{D}_1,\mathbf{R}_{22}=-I_{11}h\mathbf{D}_{10}-I_{22}\frac{4h}{L^2}\mathbf{D}_{12},\mathbf{R}_{23}=-I_{23}\frac{2}{L}\mathbf{D}_1,$$
$$\mathbf{R}_{24}=-I_{24}\frac{2}{Lh}\mathbf{D}_1,\mathbf{R}_{25}=-I_{25}\frac{2}{Lh}\mathbf{D}_1, \tag{A.12}$$

$$\mathbf{R}_{31}=-I_{13}h\mathbf{I},\mathbf{R}_{32}=-I_{23}\frac{2h}{L}\mathbf{D}_{11},\mathbf{R}_{33}=-I_{33}\mathbf{I},\mathbf{R}_{34}=-\frac{I_{34}}{h}\mathbf{I},\mathbf{R}_{35}=-\frac{I_{35}}{h}\mathbf{I}, \tag{A.13}$$

$$\mathbf{R}_{41}=-I_{14}h\mathbf{I},\mathbf{R}_{42}=-I_{24}\frac{2h}{L}\mathbf{D}_{11},\mathbf{R}_{43}=-I_{23}\mathbf{I},\mathbf{R}_{44}=-\frac{I_{44}}{h}\mathbf{I},\mathbf{R}_{45}=\mathbf{0}, \tag{A.14}$$

$$\mathbf{R}_{51}=-I_{15}h\mathbf{I},\mathbf{R}_{52}=-I_{25}\frac{2h}{L}\mathbf{D}_{11},\mathbf{R}_{53}=-I_{25}\mathbf{I},\mathbf{R}_{54}=\mathbf{0},\mathbf{R}_{55}=-\frac{I_{55}}{h}\mathbf{I}, \tag{A.15}$$

where $\mathbf{I}$ is an identity matrix, $\mathbf{0}$ a zero matrix, and the parameters used in Eqs. (A.6) through (A.15) can be expressed as

$$C_{11}=E^th^t+E^ch^c+E^bh^b,C_{12}=-\frac{1}{2}E^th^t\left(h^t+h^c\right)+\frac{1}{2}E^bh^b\left(h^b+h^c\right),$$

$$C_{13}=E^th^t\left(\frac{G^ch^t}{3G^t}+\frac{h^c}{2}\right)-E^bh^b\left(\frac{G^ch^b}{3G^b}+\frac{h^c}{2}\right),C_{14}=\frac{E^t\left(h^t\right)^3}{12},C_{15}=\frac{E^b\left(h^b\right)^3}{12},$$

$$C_{22}=\left(\frac{E^t}{24}\left(\left(2h^t+h^c\right)^3-\left(h^c\right)^3\right)+\frac{E^c\left(h^c\right)^3}{12}+\frac{E^bh^b}{24}\left(\left(2h^b+h^c\right)^3-\left(h^c\right)^3\right)\right),$$

$$C_{23}=E^th^t\left(\frac{G^ch^t\left(5h^t+4h^c\right)}{24G^t}+\frac{h^c\left(h^t+h^c\right)}{4}\right)+\frac{E^c\left(h^c\right)^3}{12}+E^bh^b\left(\frac{G^ch^b\left(5h^b+4h^c\right)}{24G^b}+\frac{h^c\left(h^b+h^c\right)}{4}\right),$$

$$C_{24}=\frac{E^t\left(h^t\right)^3\left(7h^t+5h^c\right)}{120},C_{25}=\frac{E^b\left(h^b\right)^3\left(7h^b+5h^c\right)}{120},$$

$$C_{33}=E^th^t\left(\frac{2}{15}\left(\frac{G^ch^t}{G^t}\right)^2+\frac{G^ch^ch^t}{3G^t}+\frac{\left(h^c\right)^2}{4}\right)+\frac{E^c\left(h^c\right)^3}{12}+E^bh^b\left(\frac{2}{15}\left(\frac{G^ch^b}{G^b}\right)^2+\frac{G^ch^ch^b}{3G^b}+\frac{\left(h^c\right)^2}{4}\right),$$

$$C_{34}=E^t\left(h^t\right)^3\left(\frac{13G^ch^t}{360G^t}+\frac{h^c}{24}\right),C_{35}=E^b\left(h^b\right)^3\left(\frac{13G^ch^b}{360G^b}+\frac{h^c}{24}\right),$$

$$C_{44} = \frac{13E^t\left(h^t\right)^5}{1260}, C_{55} = \frac{13E^b\left(h^b\right)^5}{1260},$$

$$F_{33} = G^c\left(\frac{G^c h^t}{3G^t} + h^c + \frac{G^c h^b}{3G^b}\right), F_{34} = \frac{G^c\left(h^t\right)^2}{12}, F_{35} = \frac{G^c\left(h^b\right)^2}{12},$$

$$F_{44} = \frac{G^t\left(h^t\right)^3}{30}, F_{55} = \frac{G^b\left(h^b\right)^3}{30}.$$

Data availability

Data will be made available on request.

References

[1] P. Hajela, C. Lin, Optimal design of viscoelastically damped beam structures, Appl. Mech. Rev. 44 (11S) (1991) S96–S106, https://doi.org/10.1115/1.3121378.
[2] H. Hu, S. Belouettar, M. Potier-Ferry, Review and assessment of various theories for modeling sandwich composites, Compos. Struct. 84 (3) (2008) 282–292, https://doi.org/10.1016/j.compstruct.2007.08.007.
[3] M.F. Caliri Jr, A.J.M. Ferreira, V Tita, A review on plate and shell theories for laminated and sandwich structures highlighting the Finite Element Method, Compos. Struct. 156 (2016) 63–77, https://doi.org/10.1016/j.compstruct.2016.02.036.
[4] E.M Kerwin Jr, Damping of flexural waves by a constrained viscoelastic layer, J. Acoust. Soc. Am. 31 (7) (1959) 952–962, https://doi.org/10.1121/1.1907821.
[5] R.A. DiTaranto, Theory of vibratory bending for elastic and viscoelastic layered finite-length beams, J. Appl. Mech. 32 (4) (1965) 881–886, https://doi.org/10.1115/1.3627330.
[6] R.A. DiTaranto, W. Blasingame, Composite Damping of Vibrating Sandwich Beams, J. Eng. Ind. 89 (4) (1967) 633–638, https://doi.org/10.1115/1.3610124.
[7] D.J. Mead, S Markus, The forced vibration of a three-layer, damped sandwich beam with arbitrary boundary conditions, J. Sound. Vib. 10 (2) (1969) 163–175, https://doi.org/10.1016/0022-460X(69)90193-X.
[8] D.J. Mead, S Markus, Loss factors and resonant frequencies of encastre damped sandwich beams, J. Sound. Vib. 12 (1) (1970) 99–112, https://doi.org/10.1016/0022-460X(70)90050-7.
[9] D.K. Rao, Frequency and loss factors of sandwich beams under various boundary conditions, J. Mech. Eng. Sci. 20 (5) (1978) 271–282, https://doi.org/10.1243/JMES_JOUR_1978_020_047_02.
[10] D.K. Rao, Forced vibration of a damped sandwich beam subjected to moving forces, J. Sound. Vib. 54 (2) (1977) 215–227, https://doi.org/10.1016/0022-460X(77)90024-4.
[11] M.W. Hyer, W.J. Anderson, R.A. Scott, Non-linear vibrations of three-layer beams with viscoelastic cores I. Theory, J. Sound. Vib. 46 (1) (1976) 121–136, https://doi.org/10.1016/0022-460X(76)90822-1.
[12] V. Oravský, Š. Markuš, O. Šimková, A new approximate method of finding the loss factors of a sandwich cantilever, J. Sound. Vib. 33 (3) (1974) 335–352, https://doi.org/10.1016/S0022-460X(74)80006-4.
[13] J.M. Lifshitz, M. Leibowitz, Optimal sandwich beam design for maximum viscoelastic damping, Int. J. Solids. Struct. 23 (7) (1987) 1027–1034, https://doi.org/10.1016/0020-7683(87)90094-1.
[14] E. Ioannides, P. Grootenhuis, An integral equation analysis of the harmonic response of three-layer beams, J. Sound. Vib. 82 (1) (1982) 63–82, https://doi.org/10.1016/0022-460X(82)90543-0.
[15] S. He, M.D. Rao, Prediction of loss factors of curved sandwich beams, J. Sound. Vib. 159 (1) (1992) 101–113, https://doi.org/10.1016/0022-460X(92)90453-5.
[16] A. Fasana, S. Marchesiello, Rayleigh-Ritz analysis of sandwich beams, J. Sound. Vib. 241 (4) (2001) 643–652, https://doi.org/10.1006/jsvi.2000.3311.
[17] C.L. Sisemore, C.M. Darvennes, Transverse vibration of elastic-viscoelastic-elastic sandwich beams: compression-experimental and analytical study, J. Sound. Vib. 252 (1) (2002) 155–167, https://doi.org/10.1006/jsvi.2001.4038.
[18] C. Cai, H. Zheng, G.R. Liu, Vibration analysis of a beam with PCLD patch, Appl. Acoust. 65 (11) (2004) 1057–1076, https://doi.org/10.1016/j.apacoust.2004.05.004.
[19] S.M.R. Khalili, N. Nemati, K. Malekzadeh, A.R. Damanpack, Free vibration analysis of sandwich beams using improved dynamic stiffness method, Compos. Struct. 92 (2) (2010) 387–394, https://doi.org/10.1016/j.compstruct.2009.08.020.
[20] A. Arikoglu, I. Ozkol, Vibration analysis of composite sandwich beams with viscoelastic core by using differential transform method, Compos. Struct. 92 (12) (2010) 3031–3039, https://doi.org/10.1016/j.compstruct.2010.05.022.
[21] M. Hamdaoui, G. Robin, M. Jrad, E.M. Daya, Optimal design of frequency dependent three-layered rectangular composite beams for low mass and high damping, Compos. Struct. 120 (2015) 174–182, https://doi.org/10.1016/j.compstruct.2014.09.062.
[22] M. Hamdaoui, K.S. Ledi, G. Robin, E.M. Daya, Identification of frequency-dependent viscoelastic damped structures using an adjoint method, J. Sound. Vib. 453 (2019) 237–252, https://doi.org/10.1016/j.jsv.2019.04.022.
[23] D.K. Rao, Vibration of short sandwich beams, J. Sound. Vib. 52 (2) (1977) 253–263, https://doi.org/10.1016/0022-460X(77)90644-7.
[24] D.J. Mead, S Markus, Coupled flexural, longitudinal and shear wave motion in two- and three-layered damped beams, J. Sound. Vib. 99 (4) (1985) 501–519, https://doi.org/10.1016/0022-460X(85)90537-1.
[25] R. Rikards, Finite element analysis of vibration and damping of laminated composites, Compos. Struct. 24 (3) (1993) 193–204, https://doi.org/10.1016/0263-8223(93)90213-A.
[26] K.Y. Lam, L. Chun, Dynamics response of a simply supported sandwich beam subjected to impulsive loading, Compos. Struct. 27 (3) (1994) 331–337, https://doi.org/10.1016/0263-8223(94)90092-2.
[27] M. Ganapathi, B.P. Patel, P. Boisse, O. Polit, Flexural loss factors of sandwich and laminated composite beams using linear and nonlinear dynamic analysis, Compos. B Eng. 30 (3) (1999) 245–256, https://doi.org/10.1016/S1359-8368(98)00063-8.
[28] T.S. Plagianakos, D.A. Saravanos, High-order layerwise mechanics and finite element for the damped dynamic characteristics of sandwich composite beams, Int. J. Solids. Struct. 41 (24–25) (2004) 6853–6871, https://doi.org/10.1016/j.ijsolstr.2004.05.038.
[29] M. Tahani, Analysis of laminated composite beams using layerwise displacement theories, Compos. Struct. 79 (4) (2007) 535–547, https://doi.org/10.1016/j.compstruct.2006.02.019.
[30] H. Arvin, M. Sadighi, A.R. Ohadi, A numerical study of free and forced vibration of composite sandwich beam with viscoelastic core, Compos. Struct. 92 (4) (2010) 996–1008, https://doi.org/10.1016/j.compstruct.2009.09.047.
[31] M.A.R. Loja, J.I. Barbosa, C.M.M. Soares, Dynamic behaviour of soft core sandwich beam structures using kriging-based layerwise models, Compos. Struct. 134 (2015) 883–894, https://doi.org/10.1016/j.compstruct.2015.08.096.
[32] S. Ren, G. Zhao, A new formulation of continuous transverse shear stress field for static and dynamic analysis of sandwich beams with soft core, Int. J. Numer. Methods Eng. 121 (8) (2020) 1847–1876, https://doi.org/10.1002/nme.6289.
[33] L.N. Trefethen, Spectral methods in MATLAB, Soc. Industr. Appl. Math. (2000).
[34] M.R. Malik, T.A. Zang, M.Y. Hussaini, A spectral collocation method for the Navier-Stokes equations, J. Comput. Phys. 61 (1) (1985) 64–88, https://doi.org/10.1016/0021-9991(85)90061-0.
[35] M.O. Deville, P.F. Fischer, E.H. Mund, D.K. Gartling, High-order methods for incompressible fluid flow, Appl. Mech. Rev. 56 (3) (2003) B43, https://doi.org/10.1115/1.1566402. -B43.
[36] Y. Wang, H. Tu, G. Xu, D. Gao, A review of the application of spectral methods in computational ocean acoustics, Phys. Fluids 35 (12) (2023), https://doi.org/10.1063/5.0176116.
[37] J. Sun, L. Kari, I.L. Arteaga, A dynamic rotating blade model at an arbitrary stagger angle based on classical plate theory and the Hamilton's principle, J. Sound. Vib. 332 (5) (2013) 1355–1371, https://doi.org/10.1016/j.jsv.2012.10.030.
[38] A.H. Mohazzab, L. Dozio, A spectral collocation solution for in-plane eigenvalue analysis of skew plates, Int. J. Mech. Sci. 94 (2015) 199–210, https://doi.org/10.1016/j.ijmecsci.2015.03.008.
[39] M.J. Colbrook, L.J. Ayton, A spectral collocation method for acoustic scattering by multiple elastic plates, J. Sound. Vib. 461 (2019) 114904, https://doi.org/10.1016/j.jsv.2019.114904.
[40] M. Ji, K. Inaba, Theoretical analysis of free vibration and transient response of rectangular plate–cavity system under impact loading, J. Press. Vessel. Technol. 145 (3) (2023) 031402, https://doi.org/10.1115/1.4062121.
[41] M. Ji, Y. Sekiguchi, K. Inaba, M. Naito, C. Sato, Forward and inverse analysis of transient responses for a cantilevered rectangular plate under normal and oblique impact loadings, Int. J. Impact. Eng. 174 (2023) 104514, https://doi.org/10.1016/j.ijimpeng.2023.104514.
[42] P.O. Mattei, A two-dimensional Tchebycheff collocation method for the study of the vibration of a baffled fluid-loaded rectangular plate, J. Sound. Vib. 196 (4) (1996) 407–427, https://doi.org/10.1006/jsvi.1996.0492.
[43] M.S. Sari, E.A. Butcher, Free vibration analysis of rectangular and annular Mindlin plates with undamaged and damaged boundaries by the spectral collocation method, J. Vib. Control 18 (11) (2012) 1722–1736, https://doi.org/10.1177/1077546311422242.
[44] M. Sari, M. Nazari, E.A. Butcher, Effects of damaged boundaries on the free vibration of Kirchhoff plates: comparison of perturbation and spectral collocation

solutions, J. Comput. Nonlinear Dynam. 7 (1) (2012) 011011, https://doi.org/10.1115/1.4004808.
[45] C. Wang, L. Huang, Time-domain simulation of acoustic wave propagation and interaction with flexible structures using Chebyshev collocation method, J. Sound. Vib. 331 (19) (2012) 4343–4358, https://doi.org/10.1016/j.jsv.2012.05.015.
[46] A.H. Mohazzab, Vibration Analysis of Composite Laminated Plates and Shells Using a Spectral Method, Dipartimento di Scienze e Tecnologie Aerospaziali, Doctoral Programme, XXVI Cycle, Politecnico di Milano, Milano, Italy, 2014. https://hdl.handle.net/10589/112282.
[47] A.H. Mohazzab, L. Dozio, A spectral collocation solution for in-plane eigenvalue analysis of skew plates, Int. J. Mech. Sci. 94 (2015) 199–210, https://doi.org/10.1016/j.ijmecsci.2015.03.008.
[48] X. Xie, H. Zheng, G Jin, Integrated orthogonal polynomials based spectral collocation method for vibration analysis of coupled laminated shell structures, Int. J. Mech. Sci. 98 (2015) 132–143, https://doi.org/10.1016/j.ijmecsci.2015.04.018.
[49] P. Tossapanon, N. Wattanasakulpong, Stability and free vibration of functionally graded sandwich beams resting on two-parameter elastic foundation, Compos. Struct. 142 (2016) 215–225, https://doi.org/10.1016/j.compstruct.2016.01.085.
[50] P. Tossapanon, N. Wattanasakulpong, Flexural vibration analysis of functionally graded sandwich plates resting on elastic foundation with arbitrary boundary conditions: chebyshev collocation technique, J. Sandw. Struct. Mater. 22 (2) (2020) 156–189, https://doi.org/10.1177/1099636217736003.
[51] Y. Dong, H. Liu, H. Hu, L. Wang, Semi-analytical and experimental studies on travelling wave vibrations of a moderately thick cylindrical shell subject to a spinning motion, J. Sound. Vib. 535 (2022) 117095, https://doi.org/10.1016/j.jsv.2022.117095.
[52] Y. Dong, H. Hu, L. Wang, A comprehensive study on the coupled multi-mode vibrations of cylindrical shells, Mech. Syst. Signal. Process. 169 (2022) 108730, https://doi.org/10.1016/j.ymssp.2021.108730.
[53] M. Ji, C. Kang, Y. Sekiguchi, M. Naito, C. Sato, Spectral collocation method for free vibration of sandwich plates containing a viscoelastic core, Compos. Struct. 337 (2024) 118024, https://doi.org/10.1016/j.compstruct.2024.118024.
[54] S.C.F. Fernandes, J. Cuartero, A.J.M. Ferreira, Using collocation with radial basis functions in a pseudospectral framework for a new layerwise shallow shell theory, J. Compos. Sci. 8 (11) (2024) 448, https://doi.org/10.3390/jcs8110448.
[55] F. Tornabene, M. Viscoti, R Dimitri, Equivalent layer-wise theory for the hygro-thermo-magneto-electro-elastic analysis of laminated curved shells, Thin-Walled Struct. 198 (2024) 111751, https://doi.org/10.1016/j.tws.2024.111751.
[56] F. Tornabene, M. Viscoti, R Dimitri, Thermo-mechanical analysis of laminated doubly-curved shells: higher order equivalent layer-wise formulation, Compos. Struct. 335 (2024) 117995, https://doi.org/10.1016/j.compstruct.2024.117995.
[57] M. Ji, K. Inaba, F. Triawan, Vibration characteristics of cylindrical shells filled with fluid based on first-order shell theory, J. Fluids. Struct. 85 (2019) 275–291, https://doi.org/10.1016/j.jfluidstructs.2019.01.017.
[58] M. Ji, Y.C. Wu, C.C. Ma, Theoretical analyses and numerical simulation of flexural vibration based on Reddy and modified higher-order plate theories for a transversely isotropic circular plate, Acta Mech. 232 (7) (2021) 2825–2842, https://doi.org/10.1007/s00707-021-02973-y.
[59] M. Ji, Y.C. Wu, C.C. Ma, Analytical solutions for in-plane dominated vibrations of transversely isotropic circular plates based on high-order theories, J. Sound. Vib. 503 (2021) 116110, https://doi.org/10.1016/j.jsv.2021.116110.
[60] M. Ji, J.J. Zhong, Y.C. Wu, Higher-order shear deformation theory for accurate prediction of vibration behavior of thick piezoelectric disks and design of efficient surface electrodes, Int. J. Solids. Struct. 290 (2024) 112669, https://doi.org/10.1016/j.ijsolstr.2024.112669.
[61] C. Shu, H. Du, Implementation of clamped and simply supported boundary conditions in the GDQ free vibration analysis of beams and plates, Int. J. Solids. Struct. 34 (7) (1997) 819–835, https://doi.org/10.1016/S0020-7683(96)00057-1.
[62] N. Mai-Duy, An effective spectral collocation method for the direct solution of high-order ODEs, Comm. Numer. Meth. Eng. 22 (6) (2006) 627–642, https://doi.org/10.1002/cnm.841.
[63] J. Blaber, B. Adair, A. Antoniou, Ncorr: open-source 2D digital image correlation matlab software, Exp. Mech. 55 (6) (2015) 1105–1122, https://doi.org/10.1007/s11340-015-0009-1.
[64] American Society for Testing and Materials, Standard Test Method For Measuring Vibration-Damping Properties of Materials, ASTM International, 2010.
[65] E. Cheynet, N. Daniotti, J.B. Jakobsen, J. Snæbjörnsson, Improved long-span bridge modeling using data-driven identification of vehicle-induced vibrations, Struct. Contr. Health Monit. 27 (9) (2020) e2574, https://doi.org/10.1002/stc.2574.
[66] K.S. Ledi, M. Hamdaoui, G. Robin, E.M. Daya, An identification method for frequency dependent material properties of viscoelastic sandwich structures, J. Sound. Vib. 428 (2018) 13–25, https://doi.org/10.1016/j.jsv.2018.04.031.
[67] T. Kimura, M. Ji, R. Onodera, Y. Sekiguchi, C. Sato, Inverse design of composite xylophone beams using finite element-based machine learning, Discov. Mech. Eng. 2 (1) (2023) 12, https://doi.org/10.1007/s44245-023-00020-9.
[68] M. Bilasse, E.M. Daya, L. Azrar, Linear and nonlinear vibrations analysis of viscoelastic sandwich beams, J. Sound. Vib. 329 (23) (2010) 4950–4969, https://doi.org/10.1016/j.jsv.2010.06.012.
[69] M. Bilasse, I. Charpentier, Y. Koutsawa, A generic approach for the solution of nonlinear residual equations. Part II: homotopy and complex nonlinear eigenvalue method, Comput. Methods Appl. Mech. Eng. 198 (49–52) (2009) 3999–4004, https://doi.org/10.1016/j.cma.2009.09.015.
[70] F. Abdoun, L. Azrar, E.M. Daya, M. Potier-Ferry, Forced harmonic response of viscoelastic structures by an asymptotic numerical method, Comput. Struct. 87 (1–2) (2009) 91–100, https://doi.org/10.1016/j.compstruc.2008.08.006.
[71] M.A. Trindade, A. Benjeddou, R. Ohayon, Modeling of frequency-dependent viscoelastic materials for active-passive vibration damping, J. Vib. Acoust. 122 (2) (2000) 169–174, https://doi.org/10.1115/1.568429.
[72] M.A. Trindade, Reduced-order finite element models of viscoelastically damped beams through internal variables projection, J. Vib. Acoust. 128 (4) (2006) 501–508, https://doi.org/10.1115/1.2202155.
[73] M.R. Haberman, Design of High Loss Viscoelastic Composites Through Micromechanical Modeling and Decision Based Materials design. Doctoral dissertation, George W. Woodruff School of Mechanical Engineering, Georgia Institute of Technology, Atlanta, 2007.
[74] M. Hamdaoui, F. Druesne, E.M. Daya, Variability analysis of frequency dependent visco-elastic three-layered beams, Compos. Struct. 131 (2015) 238–247, https://doi.org/10.1016/j.compstruct.2015.05.011.
[75] F. Druesne, M. Hamdaoui, P. Lardeur, Variability of dynamic responses of frequency dependent visco-elastic sandwich beams with material and physical properties modeled by spatial random fields, Compos. Struct. 152 (2016) 316–323, https://doi.org/10.1016/j.compstruct.2016.05.026.